

**SIZING, TESTING AND OPTIMIZATION OF A GEOTHERMAL MAIZE GRAIN  
DRYER: USE OF GEOTHERMAL-HEATED WATER**

**PATRICK KANJUKI GITU**

**J104/26619/2018**

**A Thesis Submitted in Partial Fulfilment of the Requirements for the Award of the Degree  
of Master of Science in Renewable Energy Technology in the School of Engineering and  
Architecture of Kenyatta University**

**MARCH, 2025**

**DECLARATION**

I declare that this thesis is my original work and has not been presented for award of any diploma or degree in any other University.

Signature .....

Date .....

Patrick Kanjuki Gitu  
J104/26619/2018

This thesis has been submitted for examination with our approval as the University supervisors.

Signature .....

Date .....

Dr. Booker Onyango Osodo  
Department of Energy, Gas and Petroleum Engineering  
Kenyatta University

Signature .....

Date .....

Prof. Willis Jakanyango Ambusso  
Department of Physics  
Kenyatta University

## ABSTRACT

Geothermal energy is a renewable form of energy that can be utilized for drying agricultural products like horticultural crops and grains. Utilization of geothermal energy to dry agricultural products requires the design of a properly sized geothermal crop dryer that meets the specific requirements for drying crops. In this study, the objective was to size, test, and optimize a geothermal maize dryer deployed at the Menengai Geothermal Project site in Nakuru County, Kenya. The components of the dryer consisted of a dryer cabinet, a water-to-air heat exchanger, drying trays and a fan unit specially fabricated to assess the drying time of the geothermal dryer. The study involved describing the heat transfer principles and equations to design these dryer components. The fabricated dryer was used to dry a batch of maize grain, evenly distributed between two trays, to lower the moisture content of the maize to 13% to allow for longer-term storage. The heat exchanger was used to dry air which was used as the drying medium. The sized fan unit was then used to blow the heated air over the maize grains. The geothermal water (brine) obtained from a discharging well at the Menengai Geothermal Project site provided the source of heat. The study investigated how the total drying time of the geothermal dryer varied at different grain layer depths, drying air temperatures, and air velocities. The study also sought to optimize the drying process and minimize the total drying time for the given geothermal dryer size using the Taguchi method to determine the optimal combination of the three parameters. Minitab 20 software was used for optimization and Analysis of Variance (ANOVA) was performed using R-4.2.3 software to test for significance of varying the parameters on the drying time. From the design, a geothermal maize dryer with 0.55m (L)  $\times$  0.25m (W)  $\times$  1m (H) dimensions and a drying capacity of 40kg was designed, tested, and optimized for drying maize grains to a moisture content of 13% moisture content wet bulb. The dryer had an axial fan with a power rating of 0.035kW and a heat exchanger with an overall heat transfer coefficient of 86.8 W/m<sup>2</sup>K. From analysis, drying time reduced with increased temperature from 40°C to 45°C by 30 minutes while the drying time was constant from 45°C to 50°C at 5 hours. The least drying time of 4 ½ hours was achieved with a drying air velocity of 0.5 m/s while maximum drying time of 5 ½ hours was achieved with a drying air velocity of 0.2m/s. As the grain depth was increased, the drying time increased from 4 ½ hours at 0.1m to 5 hours with grain depths of both 0.15m and 0.2m. Results for the optimal combination of the parameters using the Taguchi Method found that the optimal combination of parameters for the geothermal dryer were drying air temperature at 50°C, drying air velocity at 0.5m/s, and grain depth at 0.1m which would result in the minimum total drying time. ANOVA analysis showed that varying the drying air temperature and the drying air velocity had a significant impact on the total drying time. This study advances knowledge by presenting a systematic approach to designing and optimizing geothermal maize drying systems to enhance energy agricultural drying technology. The findings promote sustainable agriculture and food security by demonstrating geothermal energy as a cost-effective, eco-friendly alternative to fossil-fuel-powered drying. The optimized dryer benefits small-scale farmers and agribusinesses by reducing post-harvest losses and improving grain storage.

## **DEDICATION**

I dedicate this thesis to my supportive parents, my wife, Margaret, myself, and my awesome twosome, Leo and Mumbi, who are destined to conquer the world.

## **ACKNOWLEDGEMENT**

I am truly thankful to my supervisors, Dr. Osodo and Prof. Ambusso, for their selflessness, advice, and encouragement in completing this work.

I extend my gratitude to the management of Geothermal Development Company (GDC) for providing a location for my fieldwork studies and to the staff of the GDC Resource Utilization Department for their assistance.

To my wife, God bless you for always being my number one supporter, for your unwavering support and love throughout my studies. To our lovely kids, you are a blessing and my motivation, God bless you.

Finally, God, this is your doing, and I am forever grateful.

## TABLE OF CONTENTS

|  |      |
|--|------|
| DECLARATION .....                                    | ii   |
| ABSTRACT.....  | iii  |
| DEDICATION.....                                      | iv   |
| ACKNOWLEDGEMENT .....                                | v    |
| TABLE OF CONTENTS.....                               | vi   |
| LIST OF FIGURES .....                                | x    |
| LIST OF TABLES.....                                  | xii  |
| ABBREVIATIONS AND NOMENCLATURE.....                  | xiii |
| CHAPTER ONE: INTRODUCTION.....                       | 1    |
| 1.1 Background .....                                 | 1    |
| 1.2 Problem Statement .....                          | 3    |
| 1.3 Justification .....                              | 4    |
| 1.4 Main Objective.....                              | 5    |
| 1.4.1 Specific Objectives.....                       | 5    |
| 1.5 Significance of the Study .....                  | 5    |
| 1.6 Scope and Limitations.....                       | 6    |
| CHAPTER TWO: LITERATURE REVIEW .....                 | 7    |
| 2.1 Thermal Drying.....                              | 7    |
| 2.2 Drying Techniques of Agricultural Products ..... | 8    |

|  |    |
|--|----|
| 2.2.1 Open-sun Drying .....                              | 8  |
| 2.2.2 Artificial Drying .....                            | 9  |
| 2.3 Grain Drying Psychometrics .....                     | 11 |
| 2.4 Mechanical Dryers .....                              | 12 |
| 2.4.1 Batch dryer .....                                  | 12 |
| 2.4.2 Continuous dryer .....                             | 14 |
| 2.4.3 Components of a Geothermal Cabinet Dryer .....     | 16 |
| 2.5 Dryer Performance Evaluation.....                    | 20 |
| 2.5.1 Drying Time .....                                  | 20 |
| 2.5.2 Optimization of Dryer Performance.....             | 23 |
| 2.6 Geothermal Dryers around the World.....              | 28 |
| 2.7 Limitations of Geothermal Drying.....                | 29 |
| 2.8 Summary of Literature Review.....                    | 31 |
| CHAPTER THREE: MATERIAL AND METHODS.....                 | 32 |
| 3.1 Study Area.....                                      | 32 |
| 3.2 Design of the Geothermal Maize Dryer Components..... | 33 |
| 3.2.1 Design of the Dryer Cabinet.....                   | 34 |
| 3.2.2 Design of a Heat Exchanger .....                   | 34 |
| 3.2.3 Design of the Fan Unit.....                        | 37 |
| 3.3 Sizing of the Dryer Components.....                  | 40 |

|   |    |
|---|----|
| 3.3.1 Dryer Cabinet Sizing .....  | 40 |
| 3.3.2 Plate Heat Exchanger Sizing .....   | 41 |
| 3.3.3 Fan Unit Sizing.....  | 41 |
| 3.4 Evaluation of Dryer Performance .....   | 41 |
| 3.4.1 Measuring Instruments .....   | 42 |
| 3.4.2 Experimental Procedure .....  | 42 |
| 3.5 Optimization of Dryer Performance.....  | 44 |
| 3.6 Statistical Analysis .....  | 46 |
| CHAPTER FOUR: RESULTS AND DISCUSSION .....  | 47 |
| 4.1 Sizing and Fabrication of the Heat Exchanger, Fan Unit and Dryer Cabinet..... | 47 |
| 4.1.1 Dryer Cabinet .....   | 47 |
| 4.1.2 Heat Exchanger.....   | 48 |
| 4.1.3 Fan Unit .....  | 49 |
| 4.1.4 Fabrication and Assembly .....  | 50 |
| 4.2 Effect of the Selected Parameters on the Total Drying Time .....              | 52 |
| 4.2.1 Unloaded Dryer .....  | 52 |
| 4.2.2 Effect of Drying Air Temperature .....                                      | 57 |
| 4.2.3 Effect of Air Velocity .....  | 59 |
| 4.2.4 Effect of Grain Layer Depth.....  | 60 |
| 4.3 Optimization and Analysis of Variance (ANOVA).....                            | 62 |

|   |    |
|---|----|
| 4.3.1 Optimum Combination of Drying Air Temperature, Drying Air Velocity, and Grain Layer Depth ..... | 62 |
| 4.3.2 Analysis of Variance (ANOVA) .....  | 67 |
| CHAPTER FIVE: CONCLUSION AND RECOMMENDATIONS .....  | 69 |
| 5.1 Conclusion.....   | 69 |
| 5.2 Recommendations .....   | 70 |
| REFERENCES .....  | 71 |
| APPENDICES .....  | 76 |
| Appendix I: Results of Dryer Performance.....   | 76 |
| Appendix II: Dryer Optimization.....  | 78 |
| Appendix III: Publications .....  | 80 |
| Appendix IV: Definition of Terminologies.....   | 82 |
| Appendix V: Research Authorization .....  | 83 |

## LIST OF FIGURES

|  |    |
|--|----|
| Figure 2.1: Cabinet Type Geothermal Dryer Source: (Sumotarto, 2007).....   | 13 |
| Figure 2.2: Continuous Flow Grain Dryer (Popovska-Vasilevska, 2003).....   | 15 |
| Figure 2.3: Shell-and-tube heat exchanger diagram (Welty, Rorrer & Foster, 2014) .....   | 17 |
| Figure 2.4: Downhole heat exchanger (Khamala, 2016). .....   | 17 |
| Figure 2.5: Plate heat exchanger (Khamala, 2016).....  | 18 |
| Figure 2.6: Axial fan Source: (Sadaka, 2014).....  | 19 |
| Figure 2.7: Centrifugal fan Source: (Sadaka, 2014). .....  | 19 |
| Figure 3.1: Google map image showing the location of Menengai Crater with MW-03<br>highlighted in red (Source: Google Maps).....                             | 33 |
| Figure 4.1: Engineering Drawing of the Geothermal Dryer Front View.....  | 48 |
| Figure 4.2: The Fabricated Geothermal Maize Dryer (Front View).....  | 51 |
| Figure 4.3: The Fabricated Geothermal Maize Dryer showing the installed fan unit but the heat<br>exchanger is not visible (Side View) .....                  | 52 |
| Figure 4.4: Variation of Temperature for the Unloaded Geothermal Dryer.....  | 53 |
| Figure 4.5: Measured volumetric flow rate of geothermal-heated water at 0.2m/s air velocity and<br>the corresponding ambient and cabinet temperatures .....  | 54 |
| Figure 4.6: Measured volumetric flow rate of geothermal-heated water at 0.35m/s air velocity<br>and the corresponding ambient and cabinet temperatures ..... | 55 |

|  |    |
|--|----|
| Figure 4.7: Measured volumetric flow rate of geothermal-heated water at 0.5m/s air velocity and the corresponding ambient and cabinet temperatures ..... | 56 |
| Figure 4.8: Variation of the moisture content of the maize grain samples with drying time for different drying air temperatures .....                    | 58 |
| Figure 4.9: Graph that indicates the variation of the moisture content of the maize grains with drying time for different air velocities .....           | 60 |
| Figure 4.10: Variation of moisture content of the maize grains with drying time for three different grain depths .....                                   | 61 |
| Figure 4.11: Graph showing the total drying times for the L9 orthogonal array experiments .....  | 63 |
| Figure 4.12: Average SNR for individual parameters at each level .....   | 64 |
| Figure 4.13: Main effects plot for SNR for temperature, velocity, and grain depth.....   | 65 |

## LIST OF TABLES

|   |    |
|---|----|
| Table 3.1: Measuring Instruments for the Geothermal Dryer.....                      | 42 |
| Table 3.2: Parameters and Their Levels used in Evaluation of Dryer Performance..... | 43 |
| Table 3.3: Performance Evaluation of the Sized Geothermal dryer .....               | 44 |
| Table 3.4: L9 Orthogonal Array: Experimental Plan.....                              | 45 |
| Table 4.1: Effect of Air Temperature on Total Drying Time .....                     | 57 |
| Table 4.2: Effect of Drying Air Velocity on Total Drying Time.....                  | 59 |
| Table 4.3: Effect of Grain Layer Depth on Total Drying Time.....                    | 61 |
| Table 4.4: Calculated Signal to Noise Ratio for Drying Time .....                   | 63 |

## ABBREVIATIONS AND NOMENCLATURE

|                |   |
|----------------|---|
| $A_{dc}$       | Dryer cabinet cross-sectional area                |
| $A_s$          | Heat exchanger surface area                       |
| ANOVA          | Analysis of Variance                              |
| $C_p$          | Maize specific heat capacity                      |
| $C_{pa}$       | Air Specific heat capacity                        |
| $C_{pw}$       | Geothermal-heated water specific heat capacity    |
| $d_p$          | Diameter of the maize grain                       |
| EMC            | Equilibrium Moisture Content                      |
| GDC            | Geothermal Development Company                    |
| $h_a$          | Air heat transfer coefficient                     |
| $h_w$          | Geothermal-heated water heat transfer coefficient |
| kg             | Kilograms   |
| kJ             | Kilojoules  |
| $L_p$          | Drying bed length                                 |
| m              | Metres  |
| $M_a$          | Air quantity needed for drying                    |
| $\dot{m}_a$    | Air mass flow rate                                |
| $M_f$          | Dried maize final weight                          |
| $M_{gr}$       | Maize mass per tray                               |
| $\dot{m}_{gb}$ | Geothermal brine mass flow rate                   |
| $M_i$          | Initial weight of the maize                       |

|             |  |
|-------------|--|
| $L_{gr}$    | Grain layer depth                                |
| MW          | Menengai Wellpad                                 |
| $M_w$       | Moisture quantity removed from the maize         |
| $mc_{wb}$   | Moisture Content (% wet basis)                   |
| $mc_{wbi}$  | Maize initial moisture content                   |
| $mc_{wbeq}$ | Dried maize equilibrium moisture content         |
| MWe         | Megawatts of electricity                         |
| NCPB        | National Cereals and Produce Board               |
| $\Delta P$  | Pressure Drop                                    |
| $P_f$       | Fan power  |
| $P_m$       | Fan motor power                                  |
| $P_s$       | Static pressure                                  |
| $\dot{Q}$   | Heat transfer rate                               |
| $Q_{gb}$    | Heat supplied by the geothermal brine per second |
| $Q_t$       | Total heat required                              |
| RH          | Relative Humidity                                |
| $RH_i$      | Air initial humidity                             |
| $RH_f$      | Air final humidity                               |
| SNR         | Signal to Noise Ratio                            |
| $T_{a1}$    | Heat exchanger air entry temperature             |
| $T_{a2}$    | Heat exchanger air exit temperature              |
| $T_{w1}$    | Dryer cabinet geothermal water entry temperature |

|                 |   |
|-----------------|---|
| $T_{w2}$        | Dryer cabinet geothermal water exit temperature |
| $t_d$           | Total drying time                               |
| $\Delta T_{LM}$ | Logarithmic mean temperature difference         |
| $U$             | Overall heat transfer coefficient               |
| $\dot{V}$       | Volume flow rate of air                         |
| $u_{0air}$      | Velocity of air                                 |
| $V_a$           | Air volume needed for drying                    |
| $V_{gr}$        | Volume of maize grain per tray                  |
| $k$             | Copper thermal conductivity                     |
| $\delta$        | Air density                                     |
| $\mu$           | Viscosity                                       |
| $\varepsilon$   | Void space                                      |
| $u_0$           | Velocity  |
| $\rho$          | Density   |
| $\rho_{gr}$     | Maize grain bulk density                        |
| $\eta_f$        | Efficiency fan power                            |
| $\eta_m$        | Efficiency motor power                          |

## CHAPTER ONE: INTRODUCTION

### 1.1 Background

Maize holds a significant position as a major staple food in Kenya, making it a crucial component of the nation's food security efforts (Hoffmann et al., 2023). The primary regions responsible for maize production in Kenya are the Central, Rift Valley, Eastern, and Western regions (Njoroge et al., 2019). While maize farming aligns with the seasonal patterns of long and short rains, its consumption remains consistent throughout the year. However, post-harvest losses during maize storage are estimated to be between 20% and 40% in Sub-Saharan African countries (De Groote et al., 2023). Maize, being a crucial staple food in Kenya, requires efficient post-harvest management practices to minimize losses (Hoffmann et al., 2023). During harvesting, maize typically contains high moisture levels, around 20-25% wet basis (wb), which makes it susceptible to spoilage from insects and fungi (Kabeyi & Olanrewaju, 2021). To safeguard the maize grains and ensure longer storage periods, it is essential to lower the moisture content to approximately 13% using effective drying methods (Kabeyi & Olanrewaju, 2021).

Drying is a process of removing moisture from a product and entails the exchange of heat and mass between the product and its surroundings (Lund et al., 2022). When agricultural products are dried properly, they can be preserved for longer periods, thereby improving food security, and they also reduce product weight and bulk, making transportation and handling more practical (Abueluor et al., 2023). There are different drying methods, ranging from traditional open-air sun drying to mechanized form of drying (Öztürk, & Çobanoğlu, 2023). Open-air sun drying is one of the oldest methods of drying crops and it remains common due to its simplicity since crops are simply exposed directly to solar radiation and wind energy (Abueluor et al., 2023). However, this method has drawbacks, such as the need for large land areas, dependency on favorable weather conditions,

and its labor-intensive nature due to slow drying rates. It also increases the risk of spoilage and food loss due to moisture, insects, pests, dust, and soil.

Mechanized drying is a more efficient alternative to open-air sun drying as it shortens drying time, enhances product quality, and requires less land (Joshi et al., 2024). However, some mechanized drying methods, such as using presses or centrifuges, may lead to undesirable product deformation, which is not suitable for drying grains such as maize (Joshi et al., 2024). Mechanized drying often sources heat from electricity or fossil fuels which can be unreliable, polluting, or expensive (Joshi et al., 2024). These challenges can be overcome by utilizing renewable sources of energy like solar and geothermal energy which can be employed to power the mechanical dryers (Öztürk, & Çobanoğlu, 2023). Mechanized solar drying uses solar energy dryers that employ equipment that concentrate sunlight to increase temperature inside the dryer and cut energy losses, unlike open-air sun drying. It offers advantages such as reduction in running costs and reduced pollution of the environment (Sontakke & Salve, 2015). Despite these benefits, solar energy dryers are still affected by weather conditions and require costly storage and conversion systems for nighttime operation (Kabeyi & Olanrewaju, 2021). Geothermal energy dryers overcome the challenges posed by solar energy dryers. Geothermal steam can be used to dry agricultural products by spraying it directly or indirectly by using heat pumps or heat exchangers (Akhtaruzzaman et al., 2021). The continuous availability of geothermal energy throughout the year allows for year-round operation, and temperature control is possible by regulating the geothermal brine flow rate (Lund et al., 2022). Several countries have successfully utilized geothermal energy for drying various agricultural products, including Serbia dries wheat, Philippines dries copra, Mexico dries fruits, and lucerne is dried in New Zealand. This study seeks to establish the optimal air velocity, drying temperature, and grain depth for maize grain drying using geothermal energy.

## 1.2 Problem Statement

After harvesting maize, it is crucial to lower its moisture content to approximately 13% before it is stored. Failure to do so may lead to various issues such as mold development, insect infestation, germination, and contamination by aflatoxins (Stutt et al., 2023). Damaged maize due to these factors leads to food losses, and if maize contaminated by aflatoxin is consumed, it can cause food poisoning or death. To address these concerns, proper maize drying is essential.

In Kenya, industrial-scale maize drying is primarily done using fossil fuels like heavy fuel oil or electricity, both of which are expensive and environmentally harmful. Geothermal energy is an alternative for maize drying and it requires a geothermal crop dryer to effect drying. A geothermal crop dryer typically consists of a dryer cabinet, fan unit, heat exchanger, and fan unit, all of which require to be sized precisely to attain the desired moisture content in maize grains. The heat exchanger heats the drying air to the desired temperature. If not sized properly, it may lead to issues such as grain cracking from excessive heat or low rate of drying if temperatures are lower than desired. The role of the fan unit is to blow the heated air over the grains to effect drying. Oversized fan units can lead to increased energy consumption, while undersized ones may result in insufficient airflow and reduced drying rates (Joshi et al., 2024). The depth of the grain layer in the dryer is another critical factor to consider. If the layer is too thick, it may lead to rewetting of the dried grains due to saturation of the drying air. Conversely, if the layer is too thin, it may cause thermal inefficiencies due to unused energy.

Additionally, the size of the dryer cabinet is essential, as it influences the amount of grains the dryer can dry in each batch. There should be proper coordination in the sizing of all the components to achieve minimum drying time and optimal efficiency. By carefully addressing these aspects in

the design and sizing of geothermal crop dryers, efficient maize drying can be achieved, reducing food losses and ensuring safer and more sustainable storage practices in Kenya's maize production.

### **1.3 Justification**

Drying maize is crucial for preventing damage from fungi and insects that may lead to aflatoxin contamination (Stutt et al., 2023). When maize is dried properly it helps minimize losses and ensures the quality of maize is maintained, contributing to better health for consumers. Moreover, well-dried maize enhances farmers' productivity, improves the marketability of the crop, and ultimately leads to increased profits and improvement of the country's food security. A small geothermal-heated dryer presents a practical and sustainable solution to support the community, particularly small-scale farmers.

Geothermal energy is an effective and viable alternative to solar energy, fossil fuels and electricity in the industrial drying of maize. By employing a properly sized geothermal dryer, the moisture content of maize can be successfully reduced to the desired level of 13%. The optimization of the heat exchanger facilitates efficient heat transfer from the geothermal brine to the drying air, which will provide the optimal temperature needed for maize drying. Additionally, the fan unit needs to be appropriately sized to achieve the necessary air velocity, to effectively transfer heat to the maize grains and carry away the evaporated moisture. The use of an optimal grain layer depth will ensure there is uniform drying of the maize and reduce the overall drying time.

The sized geothermal dryer is expected to have minimal running costs since the geothermal energy is available from the Menengai geothermal project site. The expected initial costs for the dryer are for the purchase and fabrication of the components while the expected running costs are from the electricity used to run the fan and the labour costs for grain handling.

This project is designed to handle smaller maize batches of approximately 40 kg, making it highly convenient for local farmers who may not have access to large-scale drying facilities. The use of geothermal energy is expected to significantly reduce the drying time of maize as well as the costs of maize drying, making it a cost-effective and sustainable solution for maize drying.

#### **1.4 Main Objective**

The objective of this study was to size, test, and optimize a geothermal maize dryer for optimal drying time.

##### **1.4.1 Specific Objectives**

1. To size and fabricate the heat exchanger, fan unit and dryer cabinet for a geothermal maize grain dryer
2. To test and determine the effect of grain layer depth, drying air temperature and air velocity on the total drying time of the sized geothermal maize grain dryer
3. To establish the optimum combination of parameter levels required to achieve minimum drying time of the sized geothermal dryer

#### **1.5 Significance of the Study**

This study is significant in advancing sustainable post-harvest drying technologies by utilizing geothermal energy as a cost-effective and environmentally friendly alternative to conventional drying methods. The research enhances energy efficiency, reduces drying time, and improves maize grain quality, ensuring longer storage and reduced post-harvest losses by optimizing drying parameters.

Additionally, the study provides a practical model for integrating geothermal energy into agricultural processing, benefiting small-scale farmers, agribusinesses, and policymakers. It supports Kenya's renewable energy goals, contributes to climate resilience, and offers insights

into scalable, energy-efficient drying systems that can be adapted to other agricultural products and regions.

### **1.6 Scope and Limitations**

This research focused on the design of an efficient geothermal-powered maize grain dryer to enhance maize quality and reduce post-harvest losses. It explored the feasibility of utilizing geothermal energy as a sustainable heat source, optimizing drying conditions to improve efficiency and maintain grain quality. The dryer aimed to provide a cost-effective, environmentally friendly alternative to conventional drying methods, benefiting small-scale farmers and promoting sustainable agricultural practices by using geothermal energy. This study was limited to temperature, air velocity, and grain layer depth to determine the drying time. This research also included optimization using the Taguchi software to establish the best combination of temperature, air velocity, and grain layer depth that resulted in minimum drying time of maize to reach to 13% moisture content. Further, time and resource constraints limited the depth of experimentation, leaving opportunities for further refinements in future research. The study provided valuable insights into the potential of geothermal energy for grain drying. It contributed to the development of innovative post-harvest solutions that could enhance food security and support small-scale farmers.

## CHAPTER TWO: LITERATURE REVIEW

This chapter provides a comprehensive review of the current research on grain drying mechanisms, different types of mechanical dryers, and the utilization of geothermal dryers around the world. It also reviews the process of evaluating the performance of crop dryers and their performance is optimized.

### 2.1 Thermal Drying

Thermal drying is a process that transfers heat from the surrounding medium to the product undergoing drying. In addition to the heat transfer, there is also a concurrent mass transfer of water from the product to the surrounding medium. The main purpose of the drying process is to utilize thermal energy to elevate the temperature of the product, facilitating the evaporation and removal of moisture. This heat transfer occurs through a combination of convection, radiation, and conduction.

Conduction is a mode of heat transfer that occurs when there is direct physical contact and molecular interaction between objects. It involves the transfer of heat energy through the collision of molecules. Convection takes place in fluids, such as liquids or gases, where the heated fluid moves away from the heat source, carrying thermal energy with it. Radiation is characterized by the emission of electromagnetic waves that contribute to the overall heat transfer process during drying (Akhtaruzzaman et al., 2021). During drying, the elevated temperature provides the necessary latent heat of vaporization, causing water within the product and on its surface to evaporate. However, the rate of heat transfer to the product is limited by the thermal conductivity of its structure (Akhtaruzzaman et al., 2021). Mass transfer involves the movement of water molecules from the internal regions of the product towards its surface. This process is influenced

by the pressure difference between the moisture inside the product and the moisture in the surrounding atmosphere (Kabeyi & Olanrewaju, 2021).

## **2.2 Drying Techniques of Agricultural Products**

One of the earliest forms of preserving food is drying of agricultural products. The drying of agricultural products primarily utilizes the mode of heat transfer known as convection. During the convective heat transfer process, various factors play a crucial role in determining the drying time. These factors include the air velocity, relative humidity, and drying temperature of the drying medium. The effectiveness of both heat and mass transfer processes relies on the temperature gradient, vapor pressure, and convective coefficients present at the product's surface. As the drying air comes into contact with the product, it not only heats the product but also carries away the evaporated water in vapor form, facilitating the drying process.

After harvesting, the majority of agricultural farm products undergo processing before being consumed because they are not consumed immediately after harvesting (Popovska-Vasilevska, 2003). Food helps decrease the moisture content in these products, offering various benefits. These advantages include an enhanced shelf life, minimized risk of aflatoxin formation, and reduced mold development. Additionally, food drying contributes to cost-effective transportation and storage. The techniques utilized for food drying range from straightforward open sun drying to more complex artificial drying methods. Artificial methods include hot air drying, spray, and freeze-drying. These methods are discussed:

### **2.2.1 Open-sun Drying**

Open sun or natural drying method involves placing wet grains in the open air, where they are exposed to natural airflow and direct sunlight or shade. This traditional drying approach is commonly utilized in rural areas and for handling modest quantities of grains under favorable

weather conditions. Achieving the desired moisture content through natural drying takes a considerable amount of time, during which the grains are spread out on a drying floor and regularly stirred to ensure all grains are equally exposed to the sun (Khamala, 2016). Additionally, Tonui et al. (2014) state that there are about only four effective sun drying hours in Kenya. The researchers reported that it took about 6 days and 4 hours of open-sun drying of a maize sample to reduce its moisture content from 19.3%wb to 13.2%wb with daily drying sessions lasting about 4 hours. While studying commercial open-sun drying from traders, Groote et al. (2019) determined that it took the traders between two to seven days to dry a single batch of maize of 90kg. Kinyanjui (2013) stated that open-sun drying by small scale farmers took between 5 to 45 days to reduce the moisture content to around 13%wb.

### **2.2.2 Artificial Drying**

Artificial drying serves as a solution to the limitations posed by natural drying methods. With the advent of farming industrialization and the harvesting of larger crop quantities, along with high-yielding crops, there is a need for efficient post-harvest processes in a shorter timeframe. Unfavorable climatic conditions can further restrict the available time for drying, making artificial drying essential. This method involves subjecting grains to controlled parameters, including forced airflow and temperature, to achieve faster drying rates (Khamala, 2016). Artificial drying reduces the drying time significantly and enables the drying of larger quantities of grains within a specific timeframe.

#### **a. Hot air drying**

The hot air-drying process involves convective heat transfer, where heated air transfers heat to the grain surface. As the heat interacts with the grains, it vaporizes the water present in them. The airstream then carries away the water vapor, effectively removing moisture from the grain product.

Hot air drying is commonly employed in grain drying due to its economic efficiency, operational simplicity, and adaptability to various agricultural products (Kinyanjui, 2013).

During hot air drying, heat plays a crucial role in moisture removal from the product. However, it is essential to control the drying temperature carefully to avoid undesirable consequences on the product physical appearance and quality. Inadequate temperature control can cause grains to crack or shrink (Kinyanjui, 2013). Therefore, it is important to closely monitor and control grain drying to prevent such unwanted effects from occurring, ensuring that the quality of the dried product is maintained.

#### **b. Freeze drying**

This is a specialized vacuum drying process that involves freezing the product. During this process, the water within the product freezes and turns to ice. Subsequently, the ice is removed through a process known as sublimation, where it transitions directly from a solid to a gas without passing through the liquid state. Freeze drying is particularly suited for products that are highly susceptible to decomposition during conventional drying methods (Ghijs et al., 2017). By freezing the product and removing the water through sublimation, freeze drying preserves the integrity and quality of delicate or sensitive products, making it a preferred method for certain applications.

#### **c. Spray drying**

Crop drying by spraying is a process that involves spraying a hot air stream onto the crop to remove the moisture content from the product. It is commonly used in regions where there is high humidity or rainy seasons, which can prolong the time needed for drying crops to attain the desired moisture content for safe storage and marketing (Akhtaruzzaman et al., 2021).

## 2.3 Grain Drying Psychometrics

Drying grains requires air as the drying medium. Several properties of air that are crucial in drying and require to be known include relative humidity, air temperature, air velocity, enthalpy, and specific volume. Also, several factors in the grain such as its moisture content, quantity, and grain size need to be known. Some of these properties are highlighted:

### a. Relative humidity (RH)

Relative humidity is a measure of the saturation humidity percentage and is the ratio between the partial pressure of the water vapour in the air,  $p$  and the partial pressure of saturated water vapour at similar temperature,  $p_s$ . A hygrometer is used to measure relative humidity. Effective drying typically requires air with low relative humidity since lower relative humidity means the air can absorb more moisture.

$$RH = \frac{p}{p_s} \quad (2.1)$$

### b. Moisture content

Moisture content indicates the amount of water present in a product and is expressed as a percentage by weight on a wet or dry basis. In the case of grains, moisture content is typically measured on a wet basis. Laboratory methods like oven-drying or distillation can be used, as well as grain moisture meters. The calculation for wet basis moisture content is as follows (Helvaci et al., 2023):

$$\text{Wet basis moisture content, } mc_{wb} = \frac{M_i - M_f}{M_i} \times 100 \quad (2.2)$$

Where

$M_i$  is initial weight of the product in kg

$M_f$  is the final weight of the dried product in kg

### **c. Equilibrium moisture content**

Maize is hygroscopic like most grains, meaning they can absorb moisture from the air when the surrounding humidity is high, and can release moisture into the air when the humidity is low (Mrema et al., 2011). When the moisture content of the grains is equal to that of the surrounding air, moisture movement halts, and the grain attains equilibrium. This state is referred to as the equilibrium moisture content (EMC) (Khamala, 2016). EMC plays a crucial role in establishing the minimum moisture content to which foods can be dried under specific conditions and the maximum moisture the dried food can absorb during storage. The drying process of the grain takes place when the vapor pressure in the air is lower than that of the grain.

## **2.4 Mechanical Dryers**

The main mechanical dryers used commercially for grain drying are counterflow, concurrent flow, crossflow, and mixed flow dryers. In a crossflow dryer, drying air and grain move perpendicular to each other. In a concurrent flow dryer, both air and grain move in a similar direction, parallel to each other while in a counterflow dryer has the air flows opposite to direction of the flow of grains. The mixed flow dryer combines aspects of both concurrent flow and crossflow systems to leverage the advantages of both (Amantéa et al., 2018). The wide variety of dryer designs available makes their classification challenging. Therefore, selecting a grain dryer varies based on factors such as product to be dried, mode of heat transfer and the cost. The cost component is particularly crucial in the choice of dryer (Amantéa et al., 2018).

### **2.4.1 Batch dryer**

This type of dryer requires the loading of the product inside the dryer and allowed to dry for a specific period. The dryer is designed to allow air to flow inside the dryer interacting with the product, and exits, carrying away the moisture. Batch dryers are advantageous due to their simple

design, ease of construction and can be adapted to dry different products. Some common batch dryers are cabinet and batch-in-bin dryers (Amantéa et al., 2018).

**a. Cabinet dryer**

Cabinet dryers are designed with trays where the product is placed as drying air flows as shown in figure 2.1. Cabinet dryers are relatively small with a rectangular shape that accommodates the trays. One potential drawback of this design is that the placement of products in different locations within the dryer can lead to the products drying un-uniformly (Sumotarto, 2007).

Despite this limitation, cabinet dryers are modifiable to function as continuous dryers. By making suitable adjustments to the design and operating procedures, a cabinet dryer can be transformed into a continuous drying system, offering continuous and more uniform drying of the products as they pass through the drying chamber. This modification allows for a more efficient and streamlined drying process, making the cabinet dryer more versatile in meeting different drying requirements.

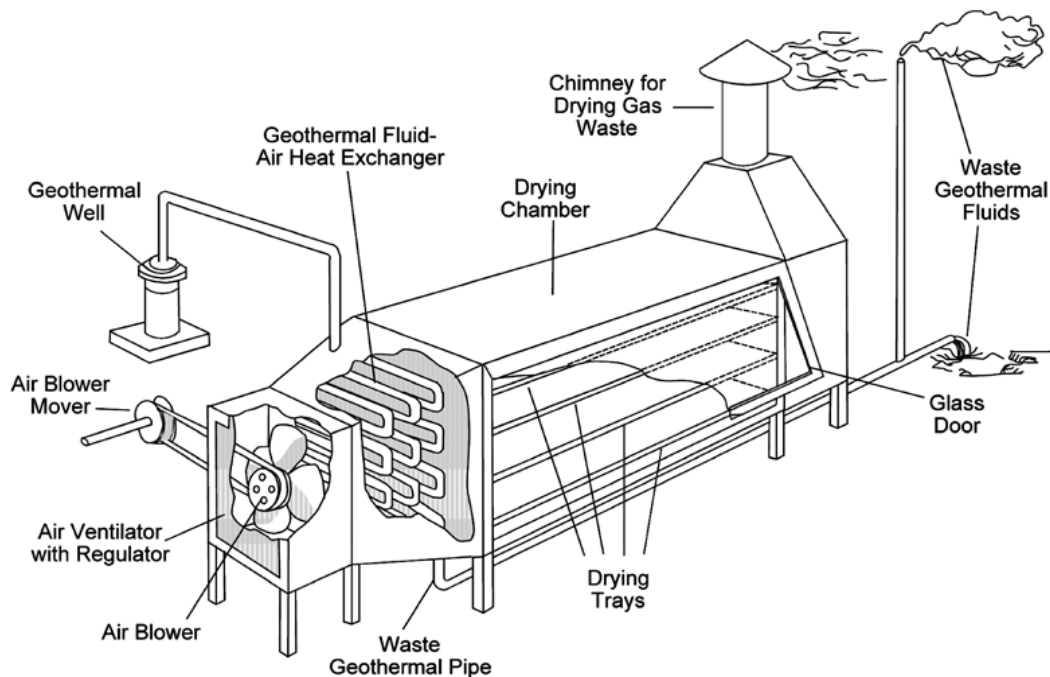


**Figure 2.1: Cabinet Type Geothermal Dryer Source: (Sumotarto, 2007)**

### ***b. Batch-in-bin dryer***

This dryer is a method of drying grains on-farm, involving the placement of grains inside a bin for the drying process. Once drying is complete, the dried grains are transferred to a separate bin where they cool down and are stored. This drying technique primarily relies on the natural airflow provided by ambient air for the drying process. However, in unfavorable weather conditions, additional heat can be introduced to expedite drying. Despite its advantages, the batch-in-bin dryer has some notable drawbacks. Regular dusting of the grains is necessary to maintain cleanliness and prevent potential contamination. Moreover, the daily loading and unloading of grains is labor-intensive and time-consuming, making it less efficient for larger quantities of grain (Khamala, 2016).

### **2.4.2 Continuous dryer**

During the drying process in continuous dryers, the product is continuously fed into and removed once it dries as shown in figure 2.2. They are designed with mechanisms that allow to be operated simultaneously with heating. These continuous dryers typically capital intensive, making them less attractive for installation. Types of continuous dryers include pneumatic, rotary, and conveyor dryers (Popovska-Vasilevska, 2003).

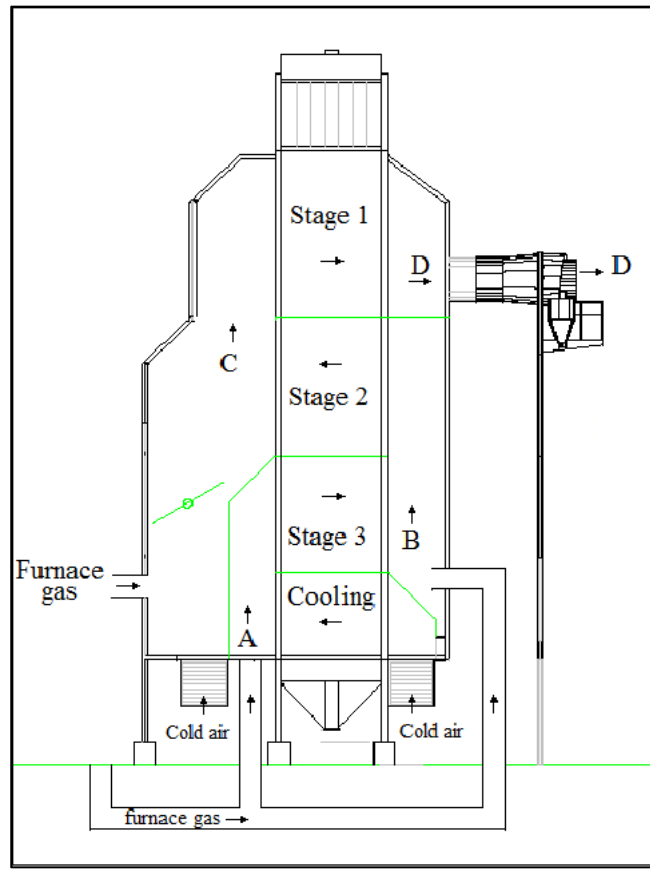


**Figure 2.2: Continuous Flow Grain Dryer (Popovska-Vasilevska, 2003)**

***a. Pneumatic dryer***

These dryers utilize a chamber or tube through which pneumatically transports the product. The velocity of the drying air is higher than the velocity of the product to facilitate the transportation of the product and also for the drying process, allowing for quick and efficient drying (Dorfeshan & Mehrzad, 2023).

***b. Rotary dryer***

This dryer is designed with a cylinder with slight inclination and is continuously rotated as the while feeding of product occurs from the upper end and moves towards the lower end where it is removed. The drying air is blown either in a concurrent direction, moving parallel to the product's

movement, or in a counter-current direction, moving opposite to the product's flow (Popovska-Vasilevska, 2003).

*c. Conveyer dryer*

These dryers have a conveyor belt where the product is placed and transported where it interacts with the drying air. This belt is usually perforated to facilitate the circulation of the drying air, and fans are used to ensure that the air reaches the entire product. The dryer's length is designed to match the residence time needed to achieve the desired moisture content of the product (Ghijs et al., 2017). This ensures that the drying process is efficient and thorough, resulting in properly dried grains with the specified moisture level.

### **2.4.3 Components of a Geothermal Cabinet Dryer**

In a typical cabinet-type geothermal crop dryer, various equipment is utilized to harness geothermal heat and direct it towards heating the air used for drying the grains. The main components of this dryer include:

**a. Heat exchanger**

This component transfers heat between two separate fluids that possess different temperatures. It consists of tubes made from high thermal conductivity materials such as aluminum or copper. In the geothermal industry, the commonly used types of heat exchangers are plate, shell-and-tube, and downhole heat exchangers (Khamala, 2016).

The shell-and-tube heat exchanger is the most common type and is shown in figure 2.3. It is designed with a set of enclosed parallel tubes within a sealed cylindrical shell. Baffles are used to support the tubes and control the desired fluid of the velocity. This arrangement allows different fluids to flow inside the tubes while the other fluid flows inside the sealed shell. However, shell-

and-tube heat exchangers have some drawbacks, such as requiring more space compared to plate heat exchangers and having lower heat efficiency. They are also more susceptible to fouling and are relatively challenging to clean and maintain (Welty, Rorrer & Foster, 2014).

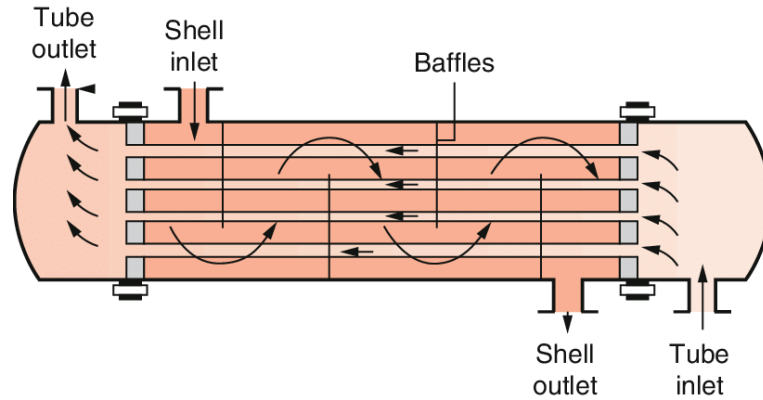


**Figure 2.3: Shell-and-tube heat exchanger diagram (Welty, Rorrer & Foster, 2014)**

Downhole heat exchangers function by incorporating a suspended pipes or tubes within a well as shown in figure 2.4. Circulation of secondary water is done through these tubes naturally or by pumping. Unlike other heat exchangers, downhole heat exchangers eliminate the need for disposing brine as it is recirculated within the well while only extracting heat. These heat exchangers are primarily utilized for heating smaller loads, such as individual homes or businesses (Khamala, 2016). This application makes them a suitable and efficient option for geothermal heating in localized settings where smaller-scale heating is required.

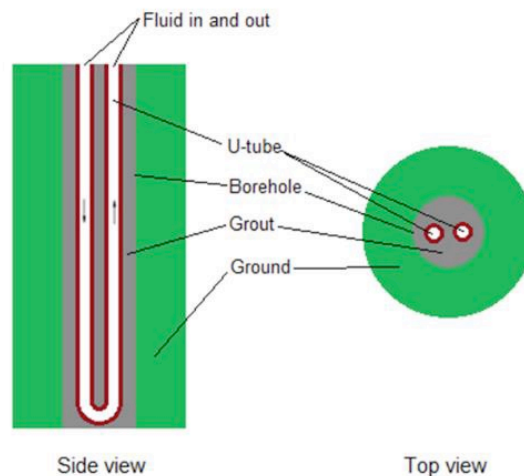


**Figure 2.4: Downhole heat exchanger (Khamala, 2016).**

The plate heat exchanger is constructed with multiple plates, each fitted with gaskets, and these plates clamping together within a frame as shown in figure 2.5. This design facilitates counter-current flow and high turbulence, enabling efficient thermal exchange in a compact space (Lund et al., 2022). One of the significant advantages of plate heat exchangers is their cost-effectiveness, as they are approximately 40% less expensive than shell-and-tube heat exchangers. Additionally, they occupy less space and can be easily expanded in size when needed. Due to these benefits, plate heat exchangers have become the predominant choice for heat exchangers in geothermal heating applications worldwide. Their ability to provide superior thermal performance and cost efficiency makes them a popular and widely adopted option in the geothermal industry.

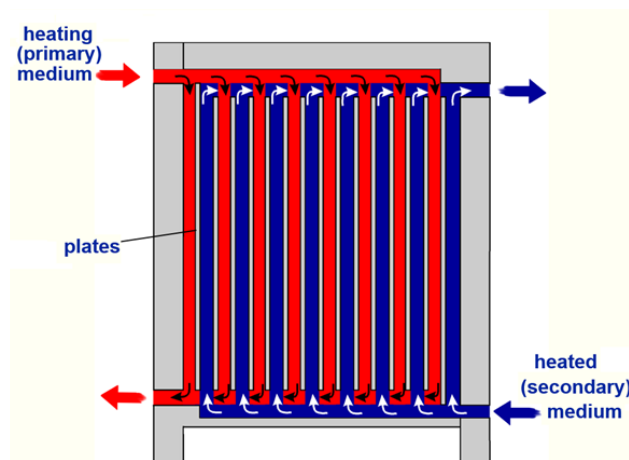


*Figure 2.5: Plate heat exchanger (Khamala, 2016)*

#### **b. Dryer cabinet**

The dryer cabinet plays a crucial role during drying as it accommodates the drying trays containing the grains to be dried. To minimize heat loss during drying, the cabinet can be insulated with good insulators such as polystyrene or polished wood (Tonui et al., 2014).

In many cases, the primary consideration in selecting the dryer cabinet is the initial cost. This is because the cost of constructing the cabinet can vary based on the material used and the insulation

method. However, it is essential to weight the options between the initial cost and the long-term efficiency and effectiveness of the cabinet in order to achieve optimal grain drying results.

### **c. Fan unit**

The fan unit in the geothermal crop dryer blows air into the cabinet for drying. The fan unit can be electricity operated or by utilizing pressure from geothermal brine flow. When choosing fans for the dryer, two main options are available: axial fans and centrifugal fans which are shown in figure 2.6 and 2.7. The selection depends on factors such as cost and volumetric airflow requirements. Axial fans are more cost-effective and provide higher airflow rates per horsepower for static pressures lower than 1120Pa compared to centrifugal fans. However, they tend to produce higher noise levels. Centrifugal fans are chosen when higher air volumes and deeper grain depth is required (Sadaka, 2014). Proper fan sizing ensures drying optimization to attain the required moisture content in the grains while minimizing energy consumption.



*Figure 2.6: Axial fan Source: (Sadaka, 2014).*



*Figure 2.7: Centrifugal fan Source: (Sadaka, 2014).*

### **d. Drying trays**

The drying trays serve as the grain holders inside the cabinet. To ensure proper airflow and efficient drying, the bottom of the trays is designed to allow for air circulation. This can be

achieved by making the bottom of the tray perforated or using wire mesh. The perforations or mesh allow the drying air to pass through and come into direct contact with the grains, promoting effective moisture removal during the drying process. Proper tray design and grain layer depth are essential in achieving uniform and efficient drying results in the geothermal crop dryer.

## **2.5 Dryer Performance Evaluation**

This research assessed the geothermal dryer performance based on its drying time. By focusing on drying time, the research aimed to evaluate how well the geothermal dryer could lower the moisture content of the grains to 13% within the desired timeframe.

### **2.5.1 Drying Time**

Drying time refers to the duration taken for the grains to reach the moisture content desired during drying. It is an essential parameter as it directly impacts the efficiency and effectiveness of the dryer. A shorter drying time would indicate higher efficiency and faster drying rates, which are favorable qualities for an optimal geothermal crop dryer. To understand and optimize the drying time, the researchers investigated the influence of three key factors: drying temperature, drying air velocity, and grain depth. These factors are known to significantly affect drying and, consequently, the drying time.

#### ***i. Drying temperature***

Increasing the drying temperature in the geothermal crop dryer directly the overall time of maize drying (Popovska-Vasilevska, 2003). However, it is essential to carefully control the drying temperature as excessively high temperatures can lead to detrimental effects on the dried maize quality. The optimal temperature for drying is influenced by several factors such as the type of dryer used, the specific type and quality of the grain being dried, and the intended use of the dried

maize. Different temperature ranges are applied for various purposes: (1) low-temperature drying: This method uses air with temperatures up to 8°C and is suitable for certain applications where the maize is not intended for human consumption but rather for specific industrial purposes, (2) medium temperature drying: For maize intended as seeds or for milling purposes, heated air with temperatures up to 43°C is used. Higher temperatures, up to 60°C, can be employed for other milling grains, (3) high-temperature drying: This approach uses heated air with temperatures up to 82°C and is typically used for maize intended as animal feed, (4) combination drying: In some cases, a combination of low and high temperatures is used for specific drying requirements (Kinyanjui, 2013; Popovska-Vasilevska, 2003).

For maize intended for human consumption and as seeds, the optimal drying temperature, according to Kinyanjui (2013), is around 43°C. Tonui et al. (2014) opined that 50°C was the highest temperature for drying maize without affecting its quality. Research by Osodo (2018) showed that the moisture removal rate significantly increased when the temperature changed from 40 to 45°C, but further temperature increases to 45-50°C and 50-55°C showed no significant impact on the moisture removal rate.

Given this information, this study used a temperature range of 40-50°C, as reported by Kinyanjui (2013) and Tonui et al. (2014), to ensure efficient drying of the maize while maintaining its quality and nutritional value. By carefully controlling the drying temperature within this range, the geothermal crop dryer aims to achieve optimal results in terms of drying efficiency and maize quality.

## *ii. Air velocity*

Achieving the desired airflow rate is crucial for efficient drying, as it helps overcome the static pressure in the dryer cabinet and ensures the desired airflow velocity to reduce the time for drying.

Increasing the air velocity to higher moisture removal from the product surface and reduced time for drying (Helvacı et al., 2023). Various studies have investigated the optimal airflow rates for thin-layer drying of maize using different drying systems. Tonui et al. (2014) found that an air velocity of between 0.20 m/s and 0.40 m/s was suitable for maize drying in a solar maize dryer. Similarly, Osodo (2018) achieved the highest drying efficiency with an air velocity of 0.41 m/s for 0.02 m grain depth. Kinyanjui (2013) demonstrated the potential of geothermal maize drying using a thin-layer drying principle with 0.5 m/s air velocity.

Based on the findings of these previous studies, the current research used an air velocity ranging from 0.2 to 0.5 m/s, based on research by Kinyanjui (2013), Osodo (2018) and Tonui et al. (2014). This selection of airflow rates is expected to enhance the efficiency of the geothermal crop dryer by providing an optimal airflow velocity for effective drying of the maize while minimizing the drying time.

### ***iii. Grain depth***

Thin-layer drying or deep bed drying methods can be used to design convective dryers. Thin-layer drying exposes all the grains uniformly to the drying air, to ensure a relatively uniform temperature is distributed throughout the grain bed under normal drying conditions. Typically, a grain bed with a thickness of up to 0.20 meters is considered a thin layer (Akhtaruzzaman et al., 2021). The drying rate in thin-layer drying is generally faster compared to deep bed drying because the drying air conditions remain relatively consistent throughout the entire grain mass.

Deep bed drying involves drying grains without totally exposing them entirely to similar drying air conditions due to the thickness of the grain bed. As a result, the temperature distribution within the grain mass varies with grain depth over time, leading to a slower drying rate compared to thin-layer drying (Akhtaruzzaman et al., 2021).

In the context of this research, the geothermal dryer was designed based on the thin-layer principle, where the grains are placed in a thin layer to ensure uniform exposure to the drying air.

### **2.5.2 Optimization of Dryer Performance**

The optimization process is crucial in achieving the best possible outcomes in various fields, including industrial processes and scientific research. Optimization aims to find the optimal values of certain parameters that lead to the desired results, whether it is minimizing production costs or maximizing production efficiency. There are several optimization processes available, each with its own strengths and applications. Some of the popular methods include the Taguchi method, Artificial Neural Network , Response Surface Methodology and Genetic Algorithm (Majdi & Esfahani, 2019).

The Taguchi method is particularly useful for optimizing a set of values and determining the most influential factors that affect a specific output parameter. By using orthogonal arrays and signal-to-noise ratios, the Taguchi method reduces the number of experimental trials needed while providing comprehensive information on the factors' effects. This leads to significant cost and time savings during the experimentation process. Artificial Neural Network is commonly used in optimization tasks that involve complex data patterns and relationships, such as pattern recognition and forecasting. Response Surface Methodology aids in determining the optimal combination of variables to achieve desired results and efficiently explore the response surface. Finally, Genetic Algorithm is an optimization technique inspired by the process of natural selection. It mimics the process of evolution to find the best solution to a problem by iteratively selecting and evolving potential solutions. Genetic Algorithms are well-suited for complex and nonlinear optimization problems (Majdi & Esfahani, 2019).

This research used the Taguchi Method due to its advantages of cost and time savings (Majdi & Esfahani, 2019). The Taguchi method is a powerful technique used to optimize the performance of systems efficiently and systematically. It involves several key steps to evaluate and improve the performance of a dryer or any other system. The first step is to establish the specific performance parameter that needs optimization, such as dryer efficiency, drying time, or drying rate. Next, the method requires identifying the independent variables that significantly impact the chosen performance parameter. For a dryer, these variables could include drying air velocity, temperature, humidity, grain depth, and moisture content. Different levels are selected for each variable to cover a range of conditions. Once the variables and levels are determined, orthogonal arrays are created to efficiently evaluate the combinations of independent variables. These arrays allow researchers to conduct the minimum number of experiments while obtaining comprehensive information on the effects of the variables. Experiments are then conducted based on the orthogonal arrays to collect data on the dryer's performance under various conditions. Each experiment represents a specific combination of independent variable levels. Signal-to-Noise Ratio (SNR) method is used to analyze the data collected. SNR helps evaluate how each independent variable affects the chosen performance parameter. It distinguishes between the desirable effects (signal) and undesirable effects or variations (noise) in the data. Finally, based on SNR analysis, the optimal combination of independent variable levels that leads to the best performance is identified. This combination maximizes the signal while minimizing the noise, resulting in improved performance of the dryer. By following these steps, the Taguchi method enables researchers and engineers to systematically identify the most influential factors and efficiently optimize the performance of the dryer or any other system. This approach not only saves time and costs but also leads to improved quality

characteristics of the system being studied (Joshi, Kumar & Baredar, 2019; Majdi & Esfahani, 2019).

The Taguchi method has found valuable applications in research on drying crops, leading to significant improvements in drying efficiency and energy consumption. Majdi and Esfahani (2019) optimized the drying of a moist rectangular material using Taguchi. By varying temperature, air velocity, and thickness ratio, the optimal combination that resulted in least energy consumption and reduced drying time was 60°C drying air temperature, 0.1 m/s air velocity, and 0.1 thickness ratio.

Joshi et al., (2019) investigated potatoes drying and with the help of the Taguchi method, they were able to identify the optimal airflow rate, air velocity, and air humidity to achieve the desired solar radiation for efficient drying. The recommended values were 39.3 m<sup>3</sup>/s airflow rate, 2.8 m/s air velocity, and 62.4% air humidity.

These examples illustrate how the Taguchi method's systematic approach to experimentation has proven effective in optimizing crop drying processes. By carefully selecting and varying the relevant parameters, researchers can achieve improved efficiency and better quality characteristics, making it a valuable tool in the field of crop drying and beyond. In the Taguchi Method, the SNR is a statistical measure used to evaluate the quality of a process. It represents the signal ratio (which is the desired output of the process) to the noise (which is any unwanted variation in the output). In general, a higher SNR indicates better process performance. There are three approaches in Taguchi Method to define the desired value for a quality characteristic:

***a. Larger is better***

In this approach, the desired value for a quality characteristic is set at the highest possible level. This is often used when the quality characteristic represents something that is desirable to have

more (Majdi & Esfahani, 2019). The objective is to increase the quality characteristic as much as possible while minimizing the variation around the target value. The formula to calculate is show in equation (2.3) (Joshi et al., 2019).

$$SNR_L = -10 \log_{10} \left( \frac{1}{n} \sum_{i=1}^n \frac{1}{y_i^2} \right) \quad (2.3)$$

***b. Nominal is better***

In this approach, the target value for a quality characteristic is set at a specific level that is considered to be the ideal or desired value. This is often used when the quality characteristic represents something that needs to be maintained at a certain level (Majdi & Esfahani, 2019). The objective is to keep the quality characteristic as close to the target value as possible while minimizing the variation around the target value. The formula to calculate is show in equation (2.4) (Joshi et al., 2019).

$$SNR_N = 10 \log_{10} \frac{\bar{y}_i^2}{s_i^2} \quad (2.4)$$

***c. Smaller is better***

In this approach, the target value for a quality characteristic is set at the lowest possible level. This is often used when the quality characteristic represents something that is undesirable to have too much of (Majdi & Esfahani, 2019). The objective is to reduce the quality characteristic as much as possible while minimizing the variation around the target value. The formula to calculate is show in equation (2.5) (Joshi et al., 2019).

$$SNR_S = -10 \log_{10} \left( \frac{1}{n} \sum_{i=1}^n y_i^2 \right) \quad (2.5)$$

Where

$y_i$  is the output to be optimized

$n$  is the number of trials for the experiment

$i$  is experiment number

Each approach requires a different set of design considerations and statistical techniques to achieve the desired quality outcome. The choice of approach is dependent on the quality characteristic being measured and the product objectives or process being designed.

After data is collected using the Taguchi Method, Analysis of Variance (ANOVA) can be employed to analyze the collected data in order to determine which factors are significant in affecting the response variable (Hunter et al., 2021). ANOVA is a statistical technique that is commonly used to analyze experimental data in order to determine whether there are significant differences between groups or treatments. It is an important tool that can provide valuable insights into the most significant factors in affecting the response variable in a Taguchi design, and can help to optimize the design for the desired outcomes. After ANOVA, Tukey's Honestly Significant Difference (Tukey's HSD) can also be used to establish which specific groups means differ significantly from each other (Hunter et al., 2021). Tukey's HSD is a statistical method used to determine whether there are significant differences between the means of multiple groups in a dataset. The purpose of Tukey's HSD is to identify which specific group means differ significantly from each other after finding a significant overall difference among the groups (Hunter et al., 2021).

In this research, smaller is better approach was used since minimizing the drying time was the desirable characteristic (Sao et al., 2022). ANOVA was also used to establish the significant factors in affecting the drying time.

## **2.6 Geothermal Dryers around the World**

Geothermal heat has been used for drying food products successfully implemented in various parts of the world, offering an eco-friendly and efficient alternative to conventional drying methods. In Menengai, Kenya, GDC installed a 6-tonne semi-commercial batch dryer in 2019 (Kulundu et al., 2022). It uses geothermal brine at 90°C that is passed through a heat exchanger, which then heats fresh water to about 78°C. A suction pump is used to blow ambient air over the heated water tubing, generating hot air at 45–55°C for the drying process. The hot air enters the drying chamber through multiple inlet points, ensuring effective moisture removal from the maize grains. A significant challenge faced by the dryer is uneven grain drying, where grains near the hot air inlet dry faster than those near the exhaust end. This can lead to inconsistent moisture content in the dried maize (Kulundu et al., 2022).

In New Zealand, geothermal steam and hot water have been utilized to dry Lucerne, resulting in the production of protein concentrate and fibrous residue. The process has proven to be commercially viable and plans for expansion are underway (Dorfeshan & Mehrzad, 2023).

Similarly, in Indonesia, a simulation was conducted to explore the use of waste geothermal brine from geothermal fields for drying maize and beans. The simulation involved a fixed tray dryer with a fluid-to-air heat exchanger, and the results highlighted the significance of geothermal brine temperature, flow rate, and airflow velocity in determining the heat transfer rate (Bagaskara et al., 2023; Sumotarto, 2007).

In Greece, geothermal energy was harnessed for tomato drying using mild temperatures and extended residence time that preserves the quality and nutritional value of the dried tomatoes (Sharmin et al., 2023).

In Indonesia, geothermal energy provides a clean and efficient source of heat for drying coconuts. Hot brine or steam from geothermal wells is used in the drying process to minimize smoke contamination. There is also the utilization of hot brine from geothermal as a drying medium to dry tea leaves and it replaces the need for industrial diesel oil. This not only reduces costs but also enhances sustainability (Bagaskara et al., 2023).

Helvacı et al. (2023) designed a geothermal dryer that utilized waste brine from a geothermal field to dry olive leaves, demonstrating a significant reduction in drying time compared to traditional open-sun drying methods. By leveraging geothermal waste heat, the system provided consistent and controlled drying conditions, leading to improved product quality, reduced moisture content, and enhanced energy efficiency.

## **2.7 Limitations of Geothermal Drying**

One of the primary limitations of geothermal energy utilization for crop drying is its location-specific nature. Geothermal resources are only available in certain areas, and therefore geothermal energy use for direct uses like crop drying is constrained to these geographically limited regions. As a result, geothermal crop drying can only be feasibly implemented in locations where suitable geothermal fields exist and where the crops to be dried can be easily accessed. In Menengai, Kenya, crop drying using geothermal is considered viable because this field is situated in Nakuru County, a significant maize-producing region. Also, Trans-Nzoia and Uasin Gishu counties, accounts for a substantial portion of the country's total annual production of maize (Khamala, 2016). The proximity of the Menengai geothermal field to major maize-producing areas makes it

an attractive option for crop drying using geothermal energy. The Menengai geothermal field is strategically located approximately 30 kilometers away from the National Cereals and Produce Board (NCPB) storage silos. This proximity positions the area as a good target market for grain drying utilizing geothermal energy as a substitute to traditional diesel-powered methods employed by NCPB.

Fouling is a notable challenge that can be encountered when utilizing geothermal energy. Fouling refers to the accumulation of materials on heat exchangers surfaces, which can lead to increased thermal resistance and significantly impact their performance. This phenomenon is of particular concern in geothermal crop drying systems, where the heat exchangers are used for thermal energy transfer from geothermal brine to the drying air.

One common cause of fouling is scaling, where dissolved materials, such as silica, tend to separate from the geothermal brine during the drying process. These dissolved materials may then remain suspended in the brine or settle as small particles, ultimately adhering to the walls of the heat exchanger. As the scaling builds up, it hampers the heat transfer efficiency of the exchanger, reducing its ability to effectively heat the air for drying and thus affecting the overall drying process.

In the case of the Menengai geothermal field, research done on MW-01 indicated that precipitation of silica occurs at temperatures below 88°C (Kinyanjui, 2013). Since the temperatures found in the Menengai field are above this threshold, this means that the risk of silica scaling was not expected to be a significant issue in the geothermal crop drying process. This was a favorable aspect that contributes to the viability of geothermal crop drying in the Menengai area.

Also, the location of this project was at the Menengai Direct Use Project site, which uses geothermal brine from MW-12 to heat fresh water via a heat exchanger for pilot projects to avoid fouling challenges. This geothermal-heated water was used for this project.

## **2.8 Summary of Literature Review**

This literature review examines the current research on grain drying mechanisms, various types of mechanical dryers, and the application of geothermal drying technologies globally. Drying techniques such as open-sun drying and artificial drying methods like hot air, freeze, and spray drying, are discussed, exploring their advantages and limitations.

The review details the psychometric factors critical to grain drying, such as relative humidity, moisture content, and which influence the drying process. It further categorizes mechanical dryers into batch and continuous dryers, explaining their operational mechanisms and suitability for different grain types. The review further highlights the components of the geothermal dryers, including heat exchangers, dryer cabinets, fan units, and drying trays, which work together to optimize drying efficiency. Performance evaluation focuses on drying time, exploring the impact of drying temperature, air velocity, and grain depth on the drying time of the geothermal dryers.

The review also discusses the optimization of dryer performance through methods like the Taguchi method, which aims to enhance drying efficiency while minimizing resource consumption. Finally, it surveys the global use of geothermal drying, showcasing successful implementations in countries such as New Zealand, Indonesia, and Greece, while noting limitations such as geographical constraints and fouling issues affecting heat exchangers. In summary, advancements in dryer design, parameter optimization, and geothermal integration offer sustainable pathways to enhance drying efficiency, reduce energy costs, and improve post-harvest quality in the agricultural sector.

## **CHAPTER THREE: MATERIAL AND METHODS**

This chapter details the study area and the designing, sizing and assembly of the geothermal maize dryer components. It then describes the process of fabricating and assembling the components to get the dryer ready for performance evaluation. The chapter also describes the process of dryer performance evaluation and optimization based on drying time.

### **3.1 Study Area**

The study was conducted in Menengai Geothermal Field, Nakuru County in Kenya. The Menengai Geothermal Field is under development with over 50 drilled wells by the Geothermal Development Company (GDC) for development of a 105Mwe power plant in the first phase (GDC, 2010). The reservoir temperatures from the drilled wells indicated temperature of over 280°C (Onyango, 2015). The drilled wells in the Menengai Geothermal Field have one-phase and two-phase flow fluids with brine flow rates ranging from 50 to 230 tonnes per hour and enthalpy ranges of 1400 to 2600 kJ/kg (Onyango, 2015). This confirms that the Menengai Geothermal Field has the needed parameters for geothermal energy direct uses. This project was undertaken at MW-03, where GDC has existing direct use projects. The brine is pumped from MW-12 and passed through a heat exchanger with fresh water to provide the heat required for the direct use projects. This project utilized the same geothermal-heated water from the heat exchanger used for the other direct use projects.

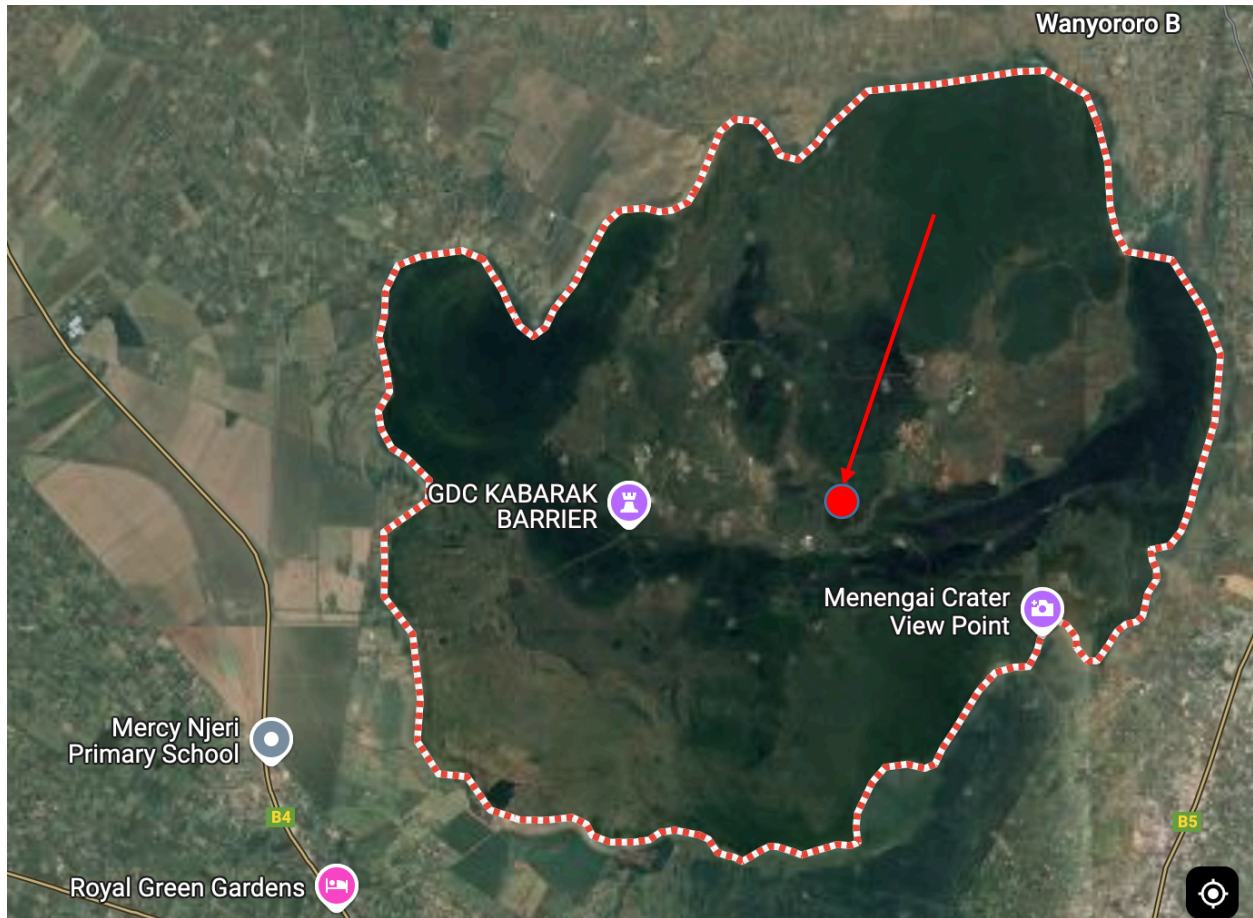


*Figure 3.1: Google map image showing the location of Menengai Crater with MW-03 highlighted in red (Source: Google Maps)*

### **3.2 Design of the Geothermal Maize Dryer Components**

The design of geothermal maize dryer was a batch-type cabinet dryer with 40kg capacity that was equally divided into two trays with each tray holding 20kg of maize grain. This weight can be handled by an individual conveniently without requiring any mechanical equipment to lift it.

### 3.2.1 Design of the Dryer Cabinet

The cross-sectional area of the trays determined the cabinet size.

#### a. Effective volume per tray

The total volume for each tray,  $V_{gr}$  was calculated by the equation (3.1) (Stephen & Emmanuel, 2009):

$$V_{gr} = \frac{m_{gr}}{\rho_{gr}} \quad (3.1)$$

Where  $m_{gr}$  is the maize grain mass per tray

$\rho_{gr}$  is the maize bulk density

#### b. Cross-sectional area of the dryer cabinet

To determine the cross-sectional area of the dryer cabinet,  $A_{dc}$  equation (3.2) was used (Stephen & Emmanuel, 2009):

$$A_{dc} = \frac{V_{gr}}{L_{gr}} \quad (3.2)$$

Where  $V_{gr}$  is the total maize volume per tray

$L_{gr}$  is the grain depth

### 3.2.2 Design of a Heat Exchanger

The selection of the counter flow design for the heat exchanger was based on its ability to achieve the most efficient heat transfer from the geothermal-heated water to the surrounding air. In a counter flow design, the fluid and the air flow in opposite directions within the heat exchanger. This arrangement allows for a high degree of heat transfer through both convective and conductive processes.

During the design process, several key parameters were calculated as highlighted:

**a. The rate of heat transfer**

Assuming zero heat loss in the heat exchanger, from the law of conservation of energy, the rate of heat transfer from the geothermal-heated water to the air is equal (Akpan et al., 2017):

$$\text{Rate of heat transfer, } \dot{Q} = \dot{m}_w C_{pw} (T_{w1} - T_{w2}) = \dot{m}_a C_{pa} (T_{a2} - T_{a1}) \quad (3.3)$$

Where

$\dot{m}_w$  and  $\dot{m}_a$  are the water and air mass flow rate respectively

$C_{pw}$  and  $C_{pa}$  are the water and air specific heat capacity respectively

$T_{w1}$  is the geothermal water temperature at heat exchanger entry

$T_{w2}$  is the geothermal water temperature at heat exchanger exit

$T_{a1}$  is the air temperature at dryer entry

$T_{a2}$  is the air temperature at dryer exit

**b. Logarithmic Mean Temperature Difference (LMTD)**

In a heat exchanger, the transfer of heat happens because of the temperature difference between the two fluids involved in the process. As the fluids flow through the heat exchanger, their temperatures change continuously along the length of the exchanger. LMTD is used to measure the average difference in temperature between the cold and hot fluids along the heat exchanger. The LMTD provides a more accurate representation of the temperature difference than using the outlet and inlet temperatures of the two fluids.

LMTD,  $\Delta T_{LM}$  is defined by (Khamala, 2016);

$$\Delta T_{LM} = \frac{(T_{w1} - T_{a2}) - (T_{w2} - T_{a1})}{\ln \left( \frac{T_{w1} - T_{a2}}{T_{w2} - T_{a1}} \right)} \quad (3.4)$$

### c. Overall heat transfer coefficient

The overall coefficient of heat transfer,  $U$  represents the overall efficiency of transfer of heat between the two fluids in the exchanger and it considers both the convection and conduction mechanisms involved in the process. It is derived from the heat transfer equations of conduction and convection (Twidell & Wyer, 2015):

$$\frac{1}{U} = \frac{r_2}{r_1 h_w} + \frac{r_2}{k} \ln\left(\frac{r_2}{r_1}\right) + \frac{1}{h_a} \quad (3.5)$$

Where

$h_w$  is the geothermal-heated water coefficient of heat transfer, W/m<sup>2</sup>K

$h_a$  is the air coefficient of heat transfer, W/m<sup>2</sup>K

$r_1$  is the tube internal diameter, m

$r_2$  is the tube external diameter, m

$k$  = thermal conductivity of tube material

### d. Surface area of the heat exchanger

To determine the effective surface area of the heat exchanger,  $A_s$  the heat exchanger performance equation is used (Khamala, 2016):

$$A_s = \frac{\dot{Q}}{\Delta T_{LM} U} = \pi D L \quad (3.6)$$

Where

$D$  is the tube diameter, m

$L$  is the tube length, m

### 3.2.3 Design of the Fan Unit

The design of the fan unit was based on the moisture required to be taken away from the maize and the amount of air required to remove the moisture.

#### a. Quantity of moisture required to be removed from the maize

The quantity of moisture that needs to be from the maize,  $M_w$  is determined by the difference in moisture contents between initial and final measurements of the maize (Akpan et al., 2017; Tonui et al., 2014):

$$M_w = M_i \frac{(mc_{wbi} - mc_{wbeq})}{(1 - mc_{wbeq})} \quad (3.7)$$

Where  $M_i$  is the maize initial mass in kg

$mc_{wbi}$  is the maize initial moisture content

$mc_{wbeq}$  is the equilibrium moisture content of the maize after drying

The moisture amount to be removed can also be calculated using the equation 3.8 (Tonui et al., 2014):

$$M_w = M_i - M_f \quad (3.8)$$

Where  $M_f$  is the final measured weight of the maize after drying in kg

Since the final weight of the maize was not known before the experiment, equation (3.7) was used.

#### b. Air needed for drying

Air needed for maize drying is calculated using the air humidity and quantity of moisture that needs to be removed (Akpan et al., 2017; Tonui et al., 2014);

$$\text{Amount of air needed for drying, } M_a = \left[ \frac{M_w}{RH_f - RH_i} \right] \quad (3.9)$$

Where  $RH_i$  is the initial humidity in kg/kg of dry air

$RH_f$  is the final humidity in kg/kg of dry air

The equation for the air volume needed for drying,  $V_a$  was calculated from eq. (3.10) (Khamala, 2016):

$$\text{Air volume needed for drying, } V_a = \frac{M_a}{\delta} \quad (3.10)$$

Where  $\delta$  is the air density, kg/m<sup>3</sup>

The equation used for air velocity,  $u_{0air}$  needed for drying was calculated from eq. (3.11) (Khamala, 2016):

$$u_{0air} = \frac{\dot{V}}{A_{dc}} \quad (3.11)$$

Where  $\dot{V}$  is the volume flow rate, m<sup>3</sup>/s

$A_{dc}$  is the dryer cabinet cross-sectional area in m<sup>2</sup>

The equation used to calculate the mass flow rate of air required to effect drying,  $m_a$  (Akpan et al., 2017) was:

$$\dot{m}_a = \delta \times u_{0air} \times A_{dc} \quad (3.12)$$

### c. Pressure drop across the drying bed

Ergun's equation is used to optimize the design of packed beds and ensure proper fluid flow and pressure distribution within the system. The equation accounts for both the kinetic energy loss due to fluid flow through the void spaces between particles and the viscous energy loss due to fluid

friction within the bed. Ergun's equation, 3.13 as used to determine the pressure drop ( $\Delta P$ ) across a packed bed with small-sized particles, is stated (Jia et al., 2015):

$$\frac{\Delta P}{L_p} = \frac{150\mu(1 - \varepsilon)^2 u_0}{\varepsilon^3 d_p^2} + \frac{1.75(1 - \varepsilon)\rho\mu^2}{\varepsilon^3 d_p} \quad (3.13)$$

Where,

$L_p$  is the length of the drying trays in m

$\mu$  is the viscosity of the fluid in kg/ms

$\varepsilon$  is the void space

$u_0$  is the velocity of the fluid in m/s

$\rho$  is the density of the fluid in kg/m<sup>3</sup>

$d_p$  is the diameter of the grain in m

#### **d. Heat supplied by the heated water**

The amount of heat supplied by the geothermal-heated water per second was given by the equation 3.14 (Kinyanjui, 2013):

$$Q_{gb} = \dot{m}_w C_{pw} (T_{b2} - T_{b1}) \quad (3.14)$$

Where

$\dot{m}_w$  is the water mass flow rate in kg/s

$C_{pw}$  is the geothermal-heated water specific heat capacity in J/kg°C

#### **e. Fan power**

The fan power,  $P_f$  determines the airflow required for the drying process. The pressure drop across drying tray is equal to the static pressure that the fan needs to overcome (Jia et al., 2015). Therefore, the equation of fan power is (Wilcke & Morey, 2015):

$$P_f = \frac{\dot{V} \times P_s}{6356 \times \eta_f} \quad (3.15)$$

Where

$\dot{V}$  is the volume flow rate of air in cfm (cubic feet per minute)

$P_s$  is the water static pressure in inches

$\eta_f$  is the efficiency of the fan (ranges between 30% to 70%)

### **3.3 Sizing of the Dryer Components**

The geothermal dryer was designed as a batch dryer, with components sized according to established design principles. The heat exchanger's surface area was calculated to efficiently transfer heat from geothermal-heated water to the surrounding air. The fan unit's sizing ensured sufficient airflow and uniform distribution. The dryer cabinet size accommodated the desired batch of maize grains for effective drying. Proper sizing maximized efficiency and maintained the quality of the final product.

#### **3.3.1 Dryer Cabinet Sizing**

The design of the cabinet was to accommodate 40kg batch of maize grain, split evenly into two trays with 20kg each. The tray dimensions were calculated using equations 3.1 and (3.2), ensuring each tray could hold the desired amount of grain. The cabinet allowed a 0.2m space above and below each tray, with a 0.2m gap between them to facilitate proper airflow during the drying process (Helvaci et al., 2023). The design allowed for manual loading without the need for mechanical lifting equipment.

### 3.3.2 Plate Heat Exchanger Sizing

The mass flow rate of air needed for drying,  $m_a$  was determined using equation (3.12) and the maximum drying air velocity was set as 0.5m/s. The rate of heat transfer,  $\dot{Q}$  was calculated using equation (3.3) to help establish the exit temperature of the geothermal-heated water. The LMTD,  $\Delta T_{LM}$  was determined using equation (3.4) while the overall heat transfer coefficient,  $U$  was determined using equation (3.5). Equations (3.4) and (3.5) were used to calculate the surface area of the heat exchanger needed to increase the temperature of drying air from ambient to peak experiment temperature of 50°C. Equation (3.6) was used to calculate the internal and external diameter and length of tubes inside the exchanger.

### 3.3.3 Fan Unit Sizing

Equation (3.13) was used to calculate the pressure drop,  $\Delta P$  using calculated values. Equation (3.15) was used to calculate the fan power,  $P_f$  using the calculated pressure drop. The cross-sectional area of the cabinet where the fan was placed and drying air velocity were used to calculate the volumetric airflow rate,  $\dot{V}$ .

### 3.4 Evaluation of Dryer Performance

After sizing, fabrication of the dryer was done by cutting, welding, and assembly of the sheet metal as per the specified dimensions. The fabricated dryer performance evaluation was based on the drying time. Initially, the dryer was run to observe its running conditions with no load for 5 hours with reading temperature readings taken at the dryer inlet, outlet and cabinet taken at 30-minute intervals.

### 3.4.1 Measuring Instruments

The measuring instruments used were tabulated in table 3.1:

*Table 3.1: Measuring Instruments for the Geothermal Dryer*

| No. | Parameter to Measured     | Instrument             | Make                  |
|-----|---------------------------|------------------------|-----------------------|
| 1.  | Moisture content          | Grain moisture meter   | Superpoint            |
| 2.  | Air velocity              | Thermo-anemometer      | Extech Instruments    |
| 3.  | Flow rate                 | Flow rate meter        | Extech Instruments    |
| 4.  | Temperature               | Thermometer            | Comark Instruments    |
| 5.  | Time                      | Digital timer          |                       |
| 6.  | Weight of the maize grain | Digital weighing scale | Endeavour Instruments |
| 7.  | Grain depth               | Ruler                  |                       |

### 3.4.2 Experimental Procedure

Before loading the dryer, it was run with no load until the required cabinet temperature level was achieved. The initial maize moisture content was measured using a grain moisture meter while the weight was recorded before loading using a digital weighing scale. The required grain layer thickness was measured using a ruler and the resultant weight of the maize grains was taken and both trays placed inside the cabinet dryer. Before the start of each experiment, the ambient temperature was recorded using a thermometer while the cabinet temperature was pre-set. The drying temperature was increased progressively from 40°C, 45°C to 50°C and the drying air velocity was increased progressively from 0.2m/s, 0.35m/s to 0.5 m/s. The grain depth was also increased progressively from 0.10m, 0.15m to 0.20 m. The axial fan was adjusted to achieve the desired drying air velocity which was measured using a thermo-anemometer while the geothermal-heated water flow rate was varied and measured using a flow rate meter to regulate the temperature

of drying air. It was then loaded with the maize grains and after loading, measurements of inlet and exit velocity, ambient, inlet and outlet temperature, were recorded using the respective measuring instruments. The maize moisture content was measured at 30-minute intervals using a digital timer until 13% moisture content was recorded. The total time taken for each experiment was measured and recorded. Table 3.2 shows the parameter levels used in the experiment (Kinyanjui, 2013; Osodo, 2018; Tonui et al., 2014):

***Table 3.2: Parameters and Their Levels used in Evaluation of Dryer Performance***

| <b>Factor</b> | <b>Parameter</b>       | <b>Units</b> | <b>Level 1</b> | <b>Level 2</b> | <b>Level 3</b> |
|---------------|------------------------|--------------|----------------|----------------|----------------|
| A             | Drying air temperature | °C           | 40             | 45             | 50             |
| B             | Drying air velocity    | m/s          | 0.2            | 0.35           | 0.5            |
| C             | Grain layer depth      | m            | 0.10           | 0.15           | 0.20           |

To determine the effect of every parameter, each parameter was varied from Level 1 to Level 3 while the other two parameters were held constant to isolate the effect of that single parameter on the outcome of the experiment. In this way, the specific effect of each parameter on the outcome of the experiment was determined. The levels to be used for the constant values were selected based on the typical values from previous experiments. For temperature, Khamala (2016) and Kinyanjui (2013) found the best temperature for maize drying for human consumption as 43 °C. Therefore, 45 °C was selected since it was the closest value to 43°C as determined by the two researchers. For air velocity, Kinyanjui (2013) and Tonui et al. (2014) established an air velocity range of 0.2 to 0.5 m/s as effective for thin-layer drying. Therefore, the air velocity selected was 0.35 m/s since it was the average value in both studies. Finally, to determine the constant value for grain layer depth, the maximum depth for thin-layer drying was 0.20m according to Akhtaruzzaman et al. (2021). Kinyanjui (2013) in his design of a geothermal grain dryer used

maximum grain depth of 0.1m for each tray. Therefore, the average value of 0.15m was selected for this research. The experiments were conducted as in table 3.3.

**Table 3.3: Performance Evaluation of the Sized Geothermal dryer**

| <b>A Effect of Drying air temperature</b> |                      |                    |                       |
|---|----------------------|--------------------|-----------------------|
| Experiment                                | Air temperature (°C) | Air velocity (m/s) | Grain layer depth (m) |
| 1   | 40                   | 0.35               | 0.15                  |
| 2   | 45                   | 0.35               | 0.15                  |
| 3   | 50                   | 0.35               | 0.15                  |
| <b>B Effect of Drying air velocity</b>    |                      |                    |                       |
| Experiment                                | Air temperature (°C) | Air velocity (m/s) | Grain layer depth (m) |
| 4   | 45                   | 0.2                | 0.15                  |
| 5   | 45                   | 0.35               | 0.15                  |
| 6   | 45                   | 0.5                | 0.15                  |
| <b>C Effect of Grain layer depth</b>      |                      |                    |                       |
| Experiment                                | Air temperature (°C) | Air velocity (m/s) | Grain layer depth (m) |
| 7   | 45                   | 0.35               | 0.1                   |
| 8   | 45                   | 0.35               | 0.15                  |
| 9   | 45                   | 0.35               | 0.2                   |

### 3.5 Optimization of Dryer Performance

The choice of optimal combination that resulted in minimum drying time was done using the Taguchi Method. An L9 orthogonal array involving 9 experiments was used to determine the drying times for each experiment as shown in table 3.4.

**Table 3.4: L9 Orthogonal Array: Experimental Plan**

| Experiment | Parameter Levels       |                     |                   | Actual Values               |                           |                       |
|------------|------------------------|---------------------|-------------------|-----------------------------|---------------------------|-----------------------|
|            | Drying Air Temperature | Drying Air Velocity | Grain Layer Depth | Drying Air Temperature (°C) | Drying Air Velocity (m/s) | Grain Layer Depth (m) |
| 1          | 1                      | 1                   | 1                 | 40                          | 0.2                       | 0.10                  |
| 2          | 1                      | 2                   | 2                 | 40                          | 0.35                      | 0.15                  |
| 3          | 1                      | 3                   | 3                 | 40                          | 0.5                       | 0.20                  |
| 4          | 2                      | 1                   | 2                 | 45                          | 0.2                       | 0.15                  |
| 5          | 2                      | 2                   | 3                 | 45                          | 0.35                      | 0.20                  |
| 6          | 2                      | 3                   | 1                 | 45                          | 0.5                       | 0.10                  |
| 7          | 3                      | 1                   | 3                 | 50                          | 0.2                       | 0.20                  |
| 8          | 3                      | 2                   | 1                 | 50                          | 0.35                      | 0.10                  |
| 9          | 3                      | 3                   | 2                 | 50                          | 0.5                       | 0.15                  |

Once the drying time for each experiment was determined, it was used to calculate the SNR.

The SNR for each parameter level was calculated to determine the optimum level for each parameter using equation (2.5). Minitab 20 statistical software main effect plots was used to confirm the results of the SNR calculations.

### **3.6 Statistical Analysis**

A three-way Analysis of Variance (ANOVA) was conducted using R-4.2.3 Programming Software to assess the individual and interactive effects of drying air temperature (40°C, 45°C, 50°C), air velocity (0.2 m/s, 0.35 m/s, 0.5 m/s), and grain depth (0.1 m, 0.15 m, 0.2 m) on the drying time.

Tukey's Honestly Significant Difference (Tukey's HSD) was also used to determine which specific groups means had a significant difference from each other. This post-hoc test enabled the identification of specific groups where drying times varied significantly.

## **CHAPTER FOUR: RESULTS AND DISCUSSION**

This chapter presents and analyzes the results that were acquired during the research process. First, the dryer cabinet, fan unit, and heat exchanger were sized and the components fabricated and assembled together. Secondly, the testing process was done and the results discussed. Finally, the optimization process was done and the optimal values for drying air velocity, drying air temperature, and grain layer depth presented and discussed.

### **4.1 Sizing and Fabrication of the Heat Exchanger, Fan Unit and Dryer Cabinet**

#### **4.1.1 Dryer Cabinet**

The maximum weight of maize to be loaded on each tray was 20kg, which was an ideal weight for a human being to load and unload without using mechanical equipment. The drying cabinet was sized based on this weight using these calculations:

Equation (3.1) was used to determine the volume needed for one tray to hold maize grain bulk of 20kg. The density of the bulk maize grain before drying was  $750 \text{ kg/m}^3$ . Therefore, the volume for one tray holding 20kg of bulk maize grain was found to be  $0.027 \text{ m}^3$ .

Equation (3.2) helped determine the cabinet tray dimensions with a maximum height of 0.2m. This area was determined to be  $0.13158\text{m}^2$  and the sides were approximated to  $0.55\text{m} \times 0.25\text{m}$ . The selected dimension of the two trays was  $0.55\text{m Length (L)} \times 0.25\text{m Width (W)} \times 0.2\text{m Height (H)}$ . The upper and lower trays were spaced by a height of 0.20m while there was a space of 0.2m from both the top section and bottom section of the dryer cabinet respectively to allow for air movement. The overall dimension of the dryer cabinet was then  $0.55\text{m (L)} \times 0.25\text{m (W)} \times 1\text{m (H)}$  was drawn using AUTOCAD 2018 as shown in figure 4.1.

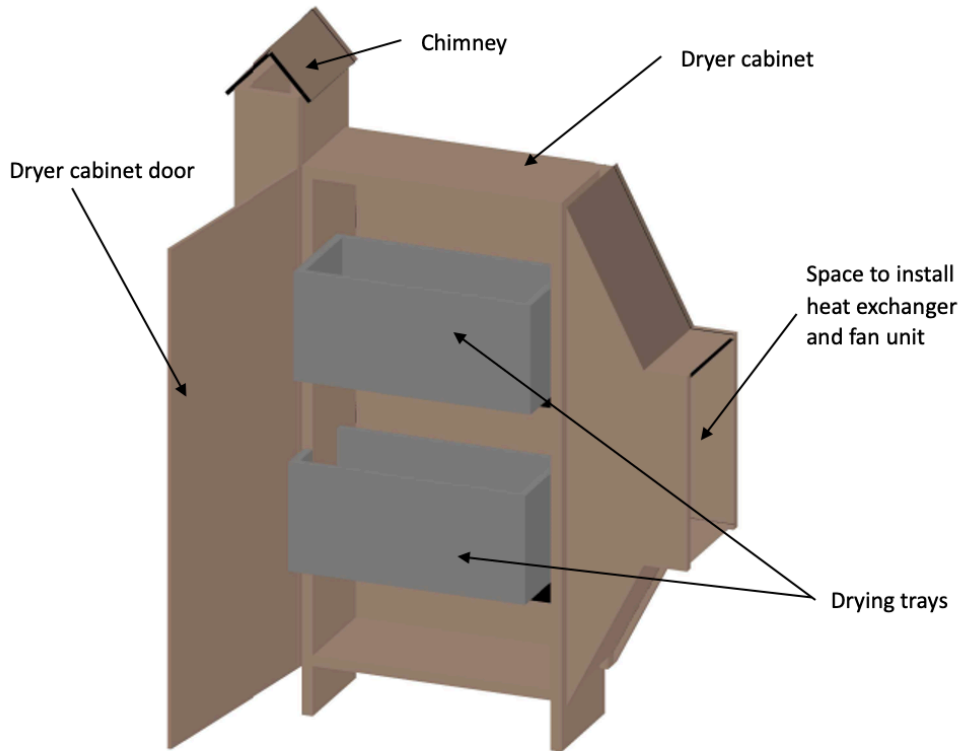


**Figure 4.1: Engineering Drawing of the Geothermal Dryer Front View**

#### **4.1.2 Heat Exchanger**

The heat exchanger dimensions were calculated using these equations. Equation (3.12) was used to calculate the mass flow rate of air needed to dry with the maximum air velocity for the experiment of 0.5m/s, the cross-sectional area, and the air density of 1.225 kg/m<sup>3</sup>. The mass flow rate of air was determined as 0.245 kg/s.

Equation (3.3) was applied to establish the heat transfer rate using the air specific heat capacity of 1005 J/kg°C, maximum temperature of the experiment of 50°C, and inlet ambient temperature of 20°C. The heat transfer rate was determined as 7386.75W. The calculated rate of heat transfer was used to calculate exit temperature for the heated water. The specific heat capacity of geothermal-heated water of 4184 J/kg°C, minimum flow rate of geothermal-heated water of 0.5kg/s and inlet

water temperatures of 78°C. The exit temperature for the heated water was determined to be 74.5 °C.

The LMTD was determined using equation (3.4) to be 39.8 °C. The overall heat transfer coefficient was calculated using equation (3.5) with internal radius,  $r_1 = 0.01m$  and external radius,  $r_2 = 0.0125m$  to give 86.8 W/m<sup>2</sup>K.

The length, surface area, internal and external diameter of the heat exchanger tubes were determined from equation (3.6). The heat exchanger tube was selected to have an internal diameter of 0.02m and a thickness of 0.0025m. The heat exchanger had a copper tube with external diameter of 0.0225m and a length of 34m calculated from equation (3.6).

#### 4.1.3 Fan Unit

Equation (3.13) was used to determine the pressure drop in the sized dryer cabinet. The void space,  $\varepsilon$  was calculated as:

$$\varepsilon = \frac{\text{Empty volume of cabinet}}{\text{Total volume of cabinet}} = \frac{0.0825}{0.1375} = 0.6$$

Other values in Ergun's equation were determined from these measurements:

$L_p$  is the length of the bed = 0.55m

$\mu$  is the fluid viscosity of air at 15°C =  $1.81 \times 10^{-5}$ kg/ms

$\varepsilon$  is the void space = 0.6

$u_0$  is the fluid velocity of air at 15°C = 0.5m/s

$\rho$  is the fluid density of air at 15°C = 1.225kg/m<sup>3</sup>

$d_p$  is the grain diameter = 9mm

The pressure drop,  $\Delta P$  was calculated using equation (3.13) with these calculated values:

$$\Delta P = 6.83 Pa$$

Equation (3.15) was used to calculate fan power,  $P_f$ . Volumetric airflow rate,  $\dot{V}$  was:

$$\dot{V} = u_0 \times A = 0.5 \times (0.25 \times 1) = 0.125 \text{ m}^3/\text{s}$$

To convert the volumetric airflow rate to cfm;

$$1 \text{ m}^3/\text{s} = 2118.9 \text{ cfm}$$

Therefore,

$$0.125 \text{ m}^3/\text{s} = 264.86 \text{ cfm}$$

To convert the pressure drop to inches of water;

$$249.082 \text{ Pa} = 1 \text{ inch of water}$$

Therefore,

$$6.83 \text{ Pa} = 0.027 \text{ inch of water}$$

$$P_f = \frac{264.86 \times 0.027}{6356 \times 0.6} = 0.002 \text{ HP}$$

To convert the horse power to kilowatts:

$$1 \text{ HP} = 0.746 \text{ kW}$$

Therefore,

$$0.002 \text{ HP} = 0.0014 \text{ kW}$$

The minimum fan power required was a 0.0014kW axial fan. A 0.035kW fan that was readily available was selected and its speed was regulated using a voltage regulator.

#### **4.1.4 Fabrication and Assembly**

The geothermal cabinet of the dimensions 0.55m (L)  $\times$  0.25m (W)  $\times$  1m (H) was fabricated using 16-gauge sheet metal (1.6mm) with a chimney to allow wet air to flow out of the cabinet. The axial fan and heat exchanger housing were also fabricated using the 16-gauge sheet metal and secured with nuts and bolts to the cabinet for easy installation and maintenance of the heat exchanger and

fan. The designed cabinet trays were fabricated with wire mesh to increase air flow and were designed to be removable for ease of loading and unloading of the maize grains as shown in figure 4.2.



***Figure 4.2: The Fabricated Geothermal Maize Dryer (Front View)***

The fan unit and the heat exchanger were then attached to the dryer cabinet. The inlet and outlet of the heat exchanger were on the bottom side for ease of connection. Figure 4.3 shows the side view of the geothermal dryer.

## 4.2 Effect of the Selected Parameters on the Total Drying Time

### 4.2.1 Unloaded Dryer

The unloaded dryer was initially run with no load for 5 hours to assess its heating capacity. The axial fan was run and the geothermal-heated water allowed to flow through the heat exchanger. The inlet (ambient) and cabinet temperature measurements were taken at 30-minute intervals and the results tabulated in Appendix I, Table A1.



*Figure 4.3: The Fabricated Geothermal Maize Dryer showing the installed fan unit but the heat exchanger is not visible (Side View)*

Figure 4.4 shows that the range of the ambient temperature was 22.3 °C to 25.1 °C while the range of cabinet temperature was from 24.3 °C to 56 °C for the five-hour experiment. The cabinet temperature range was ideal for drying maize since it was within the recommended range for drying maize for human consumption (Khamala, 2016).

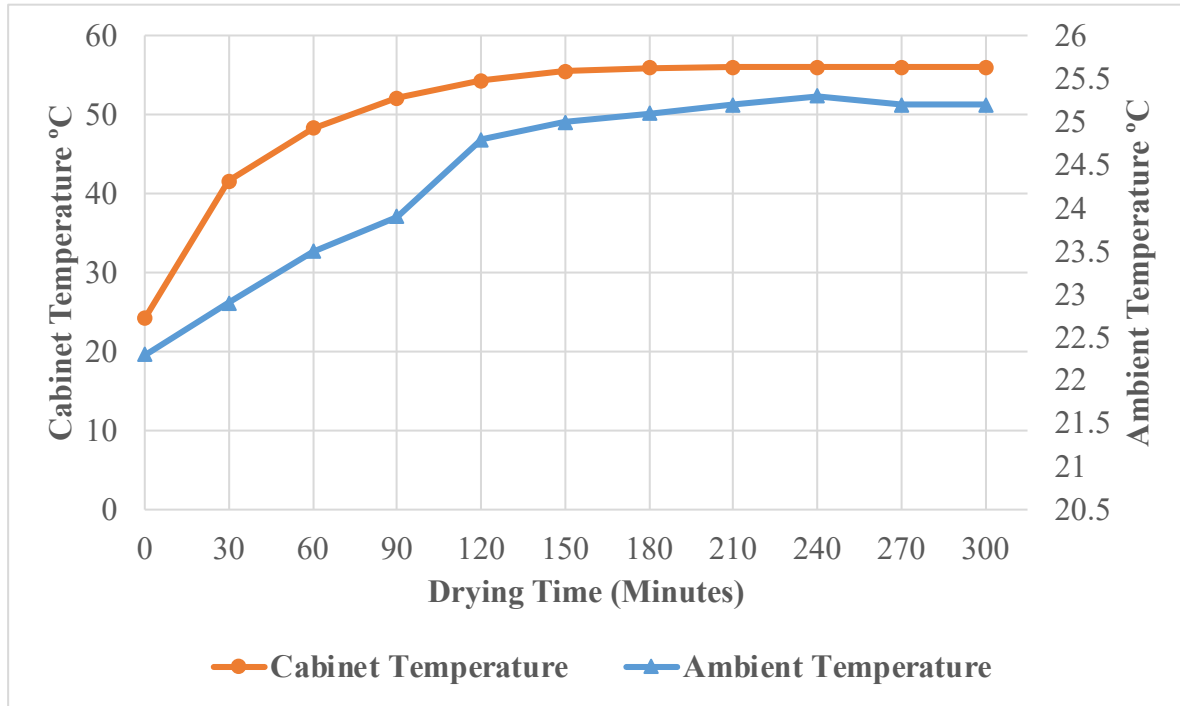


**Figure 4.4: Variation of Temperature for the Unloaded Geothermal Dryer**

Figure 4.4 shows that the cabinet temperature steadily increased over time, while the ambient temperature also increased slightly due to the time of day. During the first 30 minutes of the experiment, there was a relatively rapid increase in the cabinet temperature, which suggests that the heating system was initially warming up or stabilizing. After this initial period, the rate of increase in cabinet temperature slowed down, but still continued to rise steadily until it peaked at a maximum value of 56 °C. Further, although the ambient temperature increased slightly over time, it is not as significant as the increase in cabinet temperature, which indicated that the cabinet was able to maintain a consistent temperature, despite fluctuations in the surrounding environment.

It was important to determine the geothermal-heated water flow rates required to achieve the required cabinet temperatures for the experiment. It was possible to vary the cabinet temperature by regulating the the geothermal-heated water flow rate (Abd et al., 2018). This was tested on the unloaded dryer to determine the volumetric flow rates required to achieve the temperatures for testing the geothermal dryer. The measurements were taken at the three drying air velocities of 0.2m/s, 0.35m/s and 0.5m/s and were tabulated in Appendix I, Table A2. From the analysis, graphs were generated and they were represented in figures 4.5, 4.6 and 4.7.

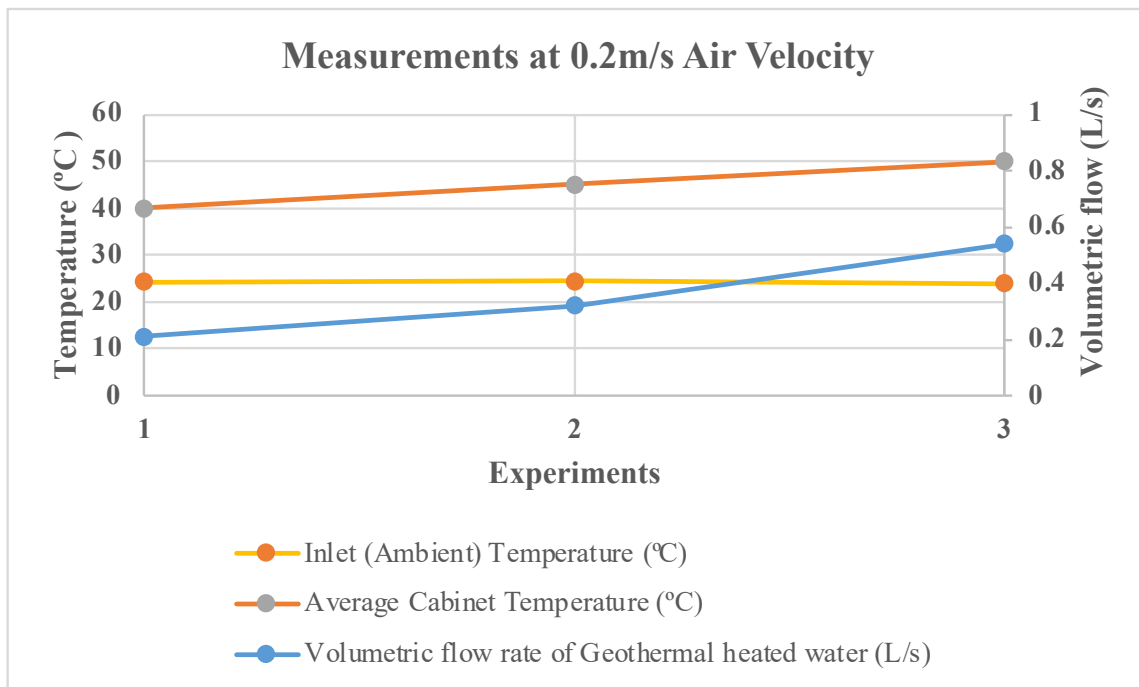


**Figure 4.5: Measured volumetric flow rate of geothermal-heated water at 0.2m/s air velocity and the corresponding ambient and cabinet temperatures**

In the three experiments shown in figure 4.5, air was blown inside the cabinet dryer at a constant air velocity of 0.2m/s to be heated up by the geothermal-heated water that flows through the heat exchanger. During the experiments, the ambient temperature ranged between 23.9 °C and 24.5 °C. As the flow rate of geothermal-heated water is increased from 0.21L/s to 0.32L/s, the cabinet temperature increases from 40 °C to 45 °C. When the flow rate is further increased to 0.54L/s, the

cabinet temperature increases to 50 °C. From the graph, as the flow rate of geothermal-heated water increases, we observe a general trend of an increase in the average cabinet temperature. This experiment provided the required geothermal-heated water flow rates required to achieve the drying temperatures of 40 °C, 45 °C and 50 °C as 0.21L/s, 0.32L/s, and 0.54L/s respectively.

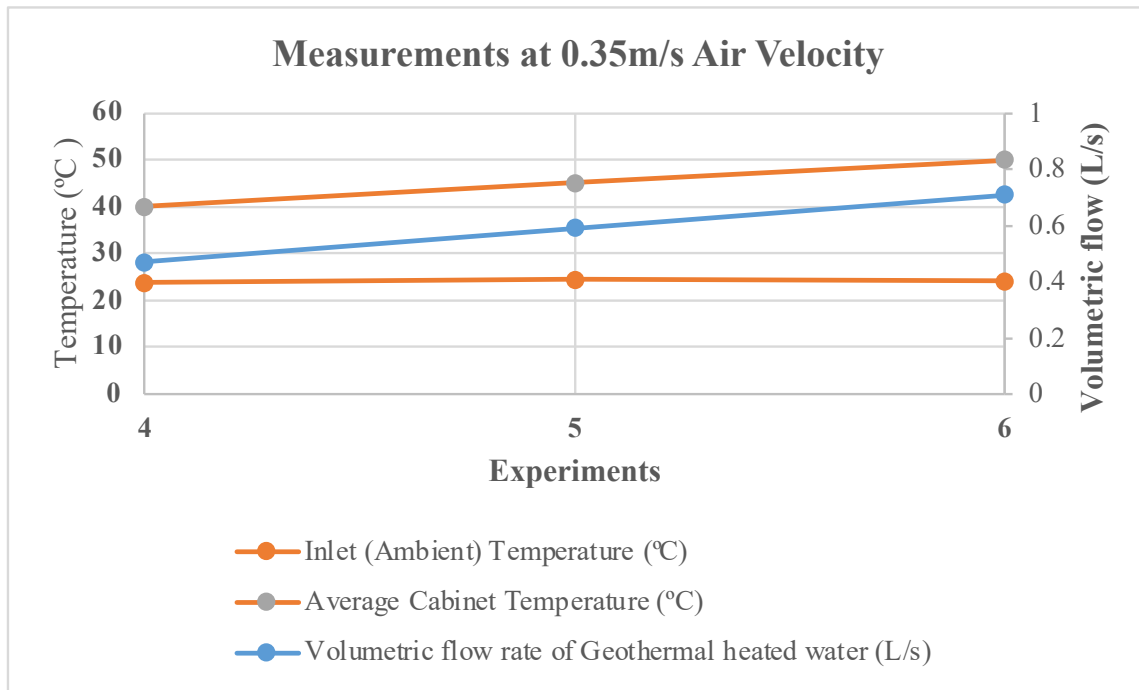


**Figure 4.6: Measured volumetric flow rate of geothermal-heated water at 0.35m/s air velocity and the corresponding ambient and cabinet temperatures**

In the three experiments shown in figure 4.6, the drying air at ambient temperature was blown inside the cabinet dryer at a constant velocity of 0.35m/s and passed through the geothermal-heated water heat exchanger. The ambient temperature of the drying air ranged from 23.8 °C to 24.4 °C and it was required to be heated to the experimental drying air temperatures of 40 °C, 45 °C, and 50 °C. From the graph, to achieve a cabinet temperature of 40 °C, the drying air was heated from an ambient temperature of 23.8 °C using a geothermal-heated water flow rate of 0.47L/s. To achieve a cabinet temperature of 45 °C, the drying air was heated from an ambient temperature of 24.4 °C using a geothermal-heated water flow rate of 0.59L/s. Similarly, to achieve a cabinet

temperature of 50 °C, the drying air was heated from an ambient temperature of 24.1 °C using a geothermal-heated water flow rate of 0.71L/s. These experiments provided the flow rates of the geothermal-heated water required to achieve the experimental cabinet temperatures at an air velocity of 0.35m/s.

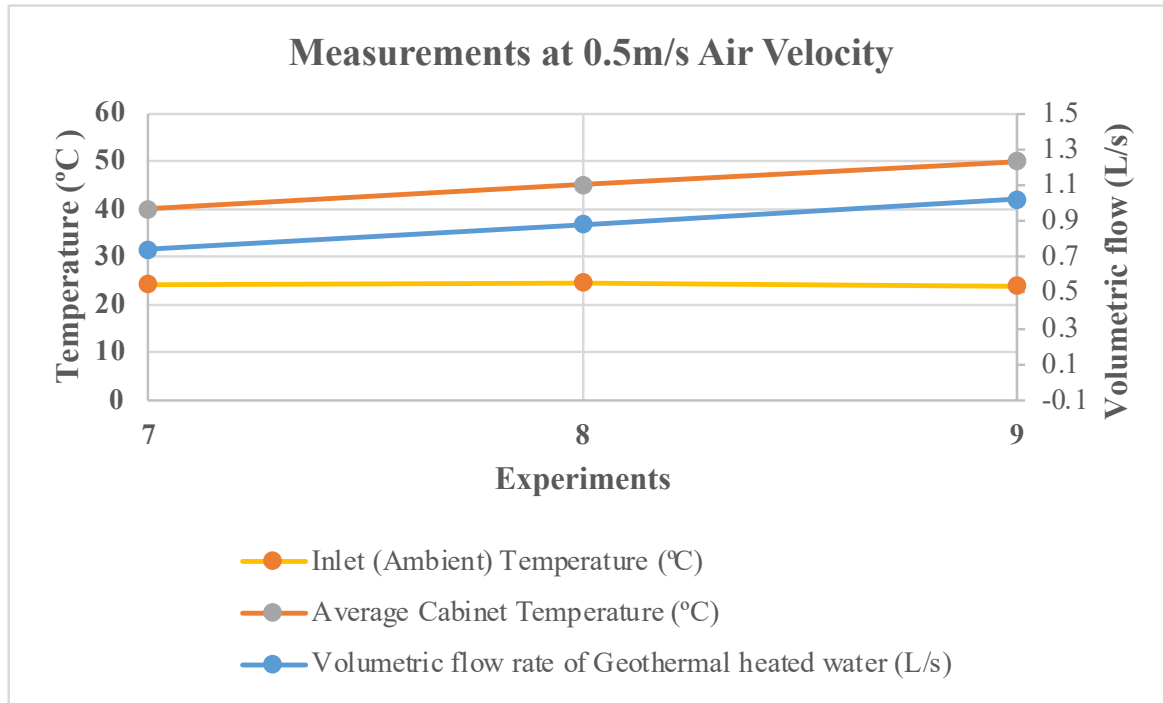


**Figure 4.7: Measured volumetric flow rate of geothermal-heated water at 0.5m/s air velocity and the corresponding ambient and cabinet temperatures**

In the three experiments shown in figure 4.7, the drying air at ambient temperature was blown inside the cabinet dryer at a constant velocity of 0.5m/s and passed through the geothermal-heated water heat exchanger. The ambient temperature of the drying air ranged from 23.9 °C to 24.6 °C and it was required to be heated to the experimental drying air temperatures of 40 °C, 45 °C, and 50 °C. From the graph, to achieve a cabinet temperature of 40 °C, the drying air was heated from an ambient temperature of 24.3 °C using a geothermal-heated water flow rate of 0.74L/s. To achieve a cabinet temperature of 45 °C, the drying air was heated from an ambient temperature of 24.6 °C using a geothermal-heated water flow rate of 0.88L/s. Similarly, to achieve a cabinet

temperature of 50 °C, the drying air was heated from an ambient temperature of 23.9 °C using a geothermal-heated water flow rate of 1.02L/s. These experiments provided the flow rates of the geothermal-heated water required to achieve the experimental cabinet temperatures at an air velocity of 0.35m/s.

These results demonstrated that it was possible to vary the cabinet temperatures using the geothermal water flow rate at different air velocities. This data is valuable for designing systems that involve geothermal heating for temperature control.

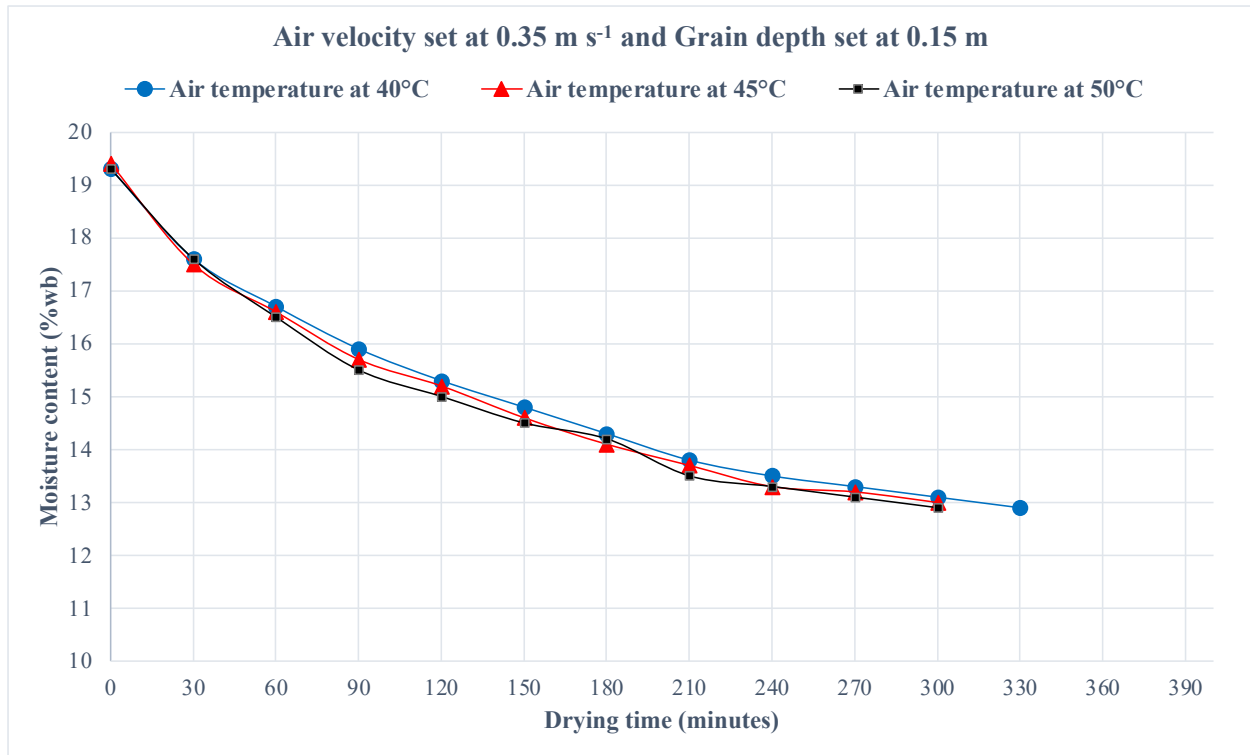
#### 4.2.2 Effect of Drying Air Temperature

Table 4.1 shows the three experiments that were conducted to determine how varying drying air temperature affected the drying time.

*Table 4.1: Effect of Air Temperature on Total Drying Time*

| <b>Experiment</b> | <b>Air Temperature (°C)</b> | <b>Air Velocity<br/>(m/s)</b> | <b>Grain Layer Depth (m)</b> |
|-------------------|-----------------------------|-------------------------------|------------------------------|
| <b>1</b>          | 40                          | 0.35                          | 0.15                         |
| <b>2</b>          | 45                          | 0.35                          | 0.15                         |
| <b>3</b>          | 50                          | 0.35                          | 0.15                         |

A grain moisture tester was used to measure the moisture content of the maize grains at 30-minute intervals until the recorded moisture content was at least 13%. The initial and final weight of each maize grain sample were also recorded. This was repeated for the three experiments and the results tabulated in Appendix I, Table A3.



**Figure 4.8: Variation of the moisture content of the maize grain samples with drying time for different drying air temperatures**

Figure 4.8 shows the moisture content variation of the maize grains with drying time for different drying air temperatures. It shows that for the three different temperatures, the moisture content reduced as the drying time increased. From the results, the least total drying time required to achieve of at least 13% wb was 300 minutes (5 hours) that was achieved at an air temperature of 45°C and 50°C. The final moisture content recorded at 45°C was marginally higher at 13%wb compared to the last moisture content recorded at 50°C of 12.9%wb. This could indicate that although the moisture content readings were taken at 30-minute intervals, the 13% moisture content was achieved at a slightly shorter time at 50°C than at 45°C. From the recorded results, increasing the drying air temperature from 40°C to 45°C reduced the total drying time by 30 minutes, which was the interval time between measurements. However, increasing the drying

temperature further from 45°C to 50°C did not result in any in the drying time reducing as both the recorded drying times were similar. Kinyanjui (2013) and Tonui et al. (2014) also reported that drying air temperature increase resulted in reducing the total drying time. Further, Osodo (2018) similarly reported that increasing the drying temperature had an effect of increasing the moisture removal rate which ultimately reduced the total drying time.

### 4.2.3 Effect of Air Velocity

Table 4.2 shows the three experiments used to determine how varying the drying air velocity affected the drying time.

*Table 4.2: Effect of Drying Air Velocity on Total Drying Time*

| <b>Experiment</b> | <b>Drying Air Velocity (m/s)</b> | <b>Drying Air Temperature (°C)</b> | <b>Grain Layer Depth (m)</b> |
|-------------------|----------------------------------|------------------------------------|------------------------------|
| <b>1</b>          | 0.2                              | 45                                 | 0.15                         |
| <b>2</b>          | 0.35                             | 45                                 | 0.15                         |
| <b>3</b>          | 0.5                              | 45                                 | 0.15                         |

A grain moisture tester was used to measure the maize grains moisture content at 30-minute intervals until the recorded moisture content was at least 13%. The initial and final weight of each maize grain were also recorded. This was repeated for the three experiments and the results tabulated in Appendix I, Table A4.

Figure 4.9 shows a graph indicating how the maize moisture content varied with drying time for different air velocities. The least total drying time required to attain a moisture content 13% was 270 minutes (4 ½ hours) which was achieved with 0.5 m/s air velocity while maximum total drying time of 330 minutes (5 ½ hours) was achieved with 0.2m/s air velocity. The recorded results

indicate that increasing the air velocity directly affected the drying time. This is an indication that the greater air velocity results in faster removal of the moisture to the atmosphere from the grain surface. Helvaci et al. (2023) reported similar results which indicated that increasing the drying air velocity caused an increase of moisture removal rate which consequently reduced the drying time. Osodo (2018) also established that 0.41m/s air velocity achieved the highest drying efficiency experiment where drying air velocity was varied from 0.21 m/s to 0.41 m/s. This indicated that an increase in air velocity had an effect of decreasing the drying time since the moisture removal rate was increased.

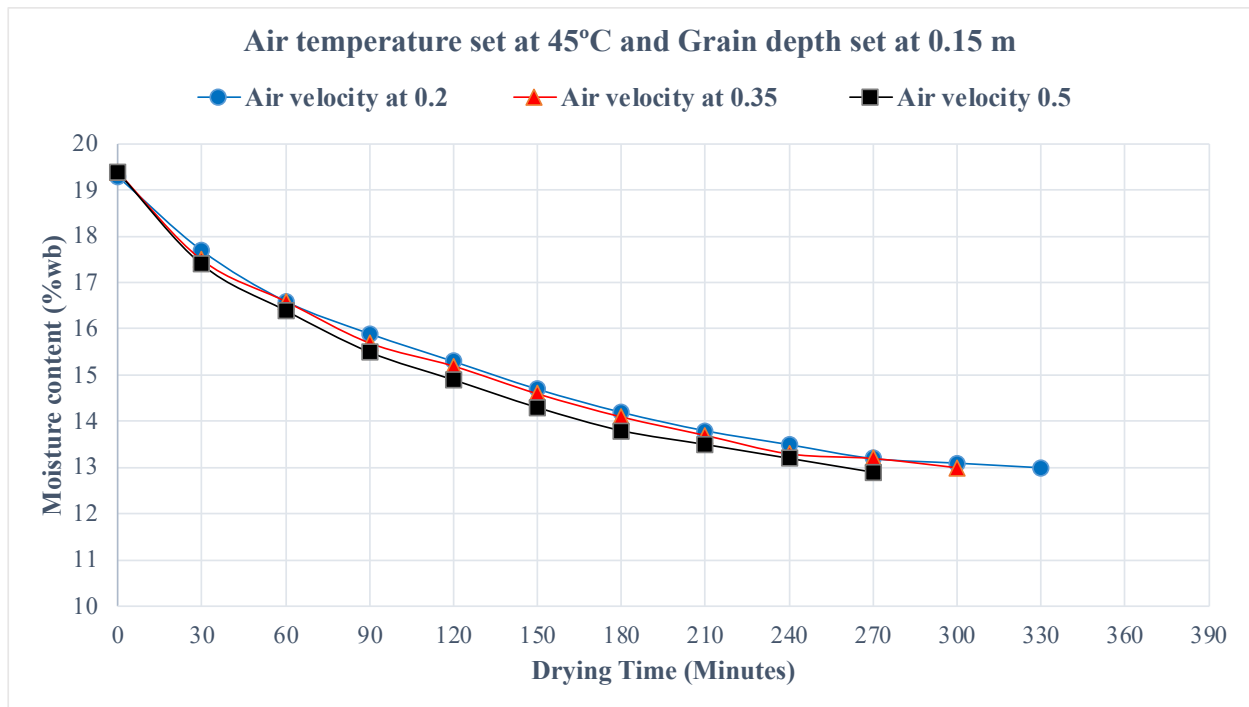


**Figure 4.9:** Graph that indicates the variation of the moisture content of the maize grains with drying time for different air velocities

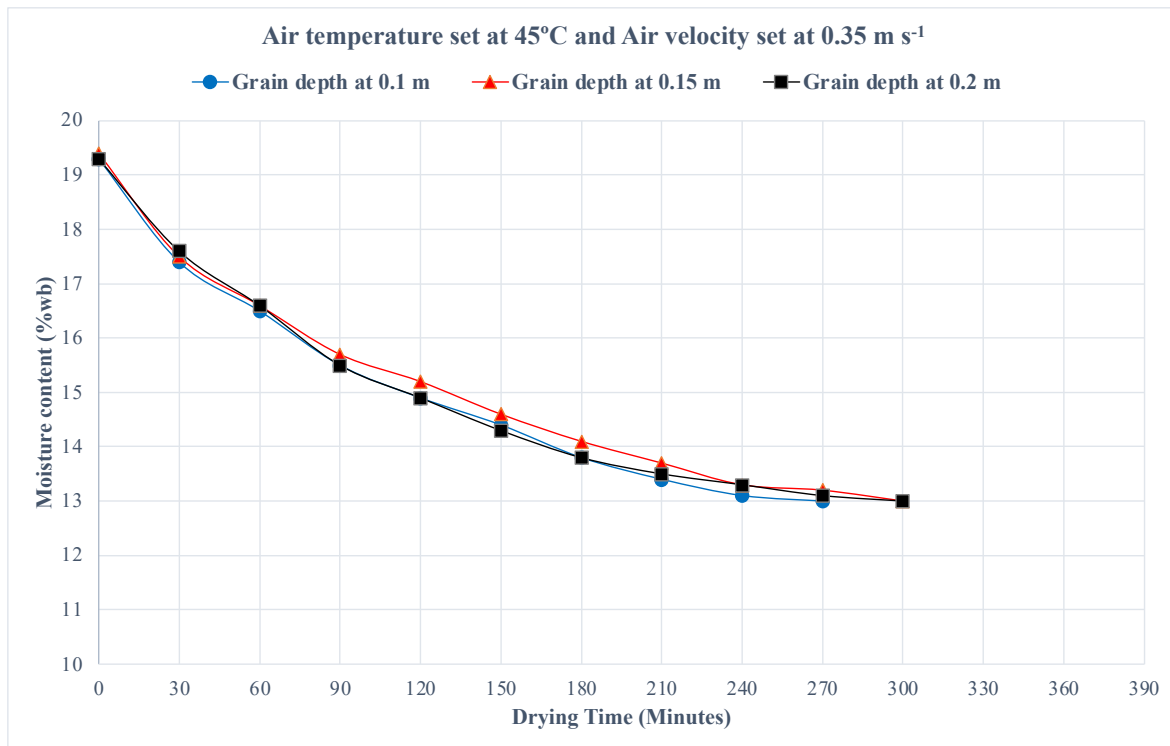
#### 4.2.4 Effect of Grain Layer Depth

Table 4.3 shows the three experiments used to determine how varying the grain layer depth affected the drying time.

**Table 4.3: Effect of Grain Layer Depth on Total Drying Time**

| Experiment | Grain Layer Depth<br>(m) | Drying Air Temperature<br>(°C) | Drying Air<br>Velocity (m/s) |
|------------|--------------------------|--------------------------------|------------------------------|
| 1          | 0.1                      | 45                             | 0.35                         |
| 2          | 0.15                     | 45                             | 0.35                         |
| 3          | 0.2                      | 45                             | 0.35                         |

A grain moisture tester was used to measure the maize grains moisture content at 30-minute intervals until the recorded moisture content was at least 13%. The initial and final weight of each maize grain were also recorded. This was repeated for the three experiments and the results tabulated in Appendix I, Table A5.



**Figure 4.10: Variation of moisture content of the maize grains with drying time for three different grain depths**

Figure 4.10 shows a graph that indicates how the moisture content of the maize varied with drying time for three different grain depths. From the graph, similar total drying times of 300 minutes (5 hours) were achieved with grain depths of 0.15m and 0.2m while minimum total drying time of 270 minutes (4 ½ hours) was achieved with a grain depth of 0.1m.

These results indicate that as the grain depth is increased, the total drying time increases because when the depth is smaller, there is lesser static pressure needed to move the air through the maize grains than when the depth is larger. This research used the thin-layer drying theory which states that a grain depth of 0.2m is the maximum value for thin-layer drying. Sadaka (2022) determined that decreasing grain depth from 0.1m to 0.0025m resulted in an increase of the drying rate of rough rice. Similar results by Sarker, Islam, and Shaheb (2012) indicated that the drying rate of potato slices increased as the thickness of the potato slices was decreased.

### **4.3 Optimization and Analysis of Variance (ANOVA)**

#### **4.3.1 Optimum Combination of Drying Air Temperature, Drying Air Velocity, and Grain Layer Depth**

Figure 4.11 shows a graph of the measured total drying time obtained from each of the nine experiments in the L9 orthogonal array shown in table 3.4. The tabulated results were tabulated in Appendix IIA, Table A1. The total drying time was used as the objective function to compute the SNR.

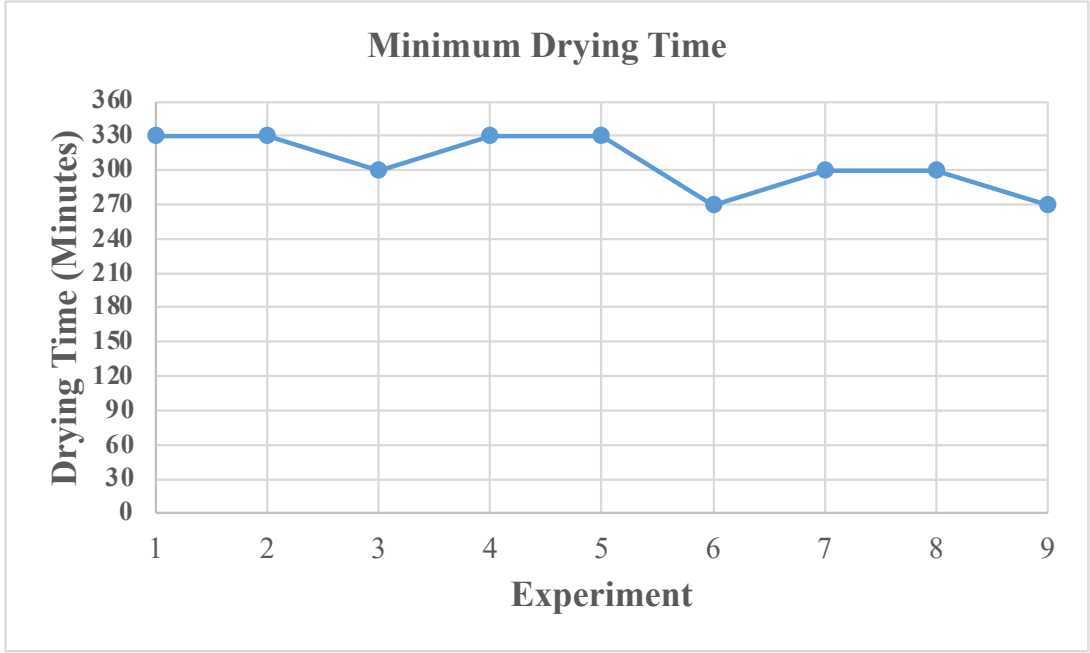


**Figure 4.11: Graph showing the total drying times for the L9 orthogonal array experiments**

The drying time is a performance measure that follows a "smaller-is-better" Taguchi approach, meaning that a shorter total drying time corresponds to better performance for the geothermal dryer. To calculate the SNR for this type of performance measure, Equation (2.5) was used.

$$SN_S = -10 \log_{10} \left( \frac{1}{n} \sum_{i=1}^n y_i^2 \right)$$

The calculated SNR values for each of the nine experiments were recorded in Table 4.4. The average SNR for each individual parameter and each level was calculated and presented in Appendix IIA, Table A2. Table 4.4 shows that the highest SNR for drying air temperature, drying air velocity, and grain layer depth are level 3 (-49.24), 3 (-48.93) and 1(-49.51) respectively.

**Table 4.4: Calculated Signal to Noise Ratio for Drying Time**

| Experiment | 1      | 2      | 3      | 4      | 5      | 6      | 7      | 8      | 9      |
|------------|--------|--------|--------|--------|--------|--------|--------|--------|--------|
| SNR        | -50.37 | -50.37 | -49.54 | -50.37 | -50.37 | -48.63 | -49.54 | -49.54 | -48.63 |

Figure 4.12 shows the parameter level with the highest SNR and the optimal level for each parameter.

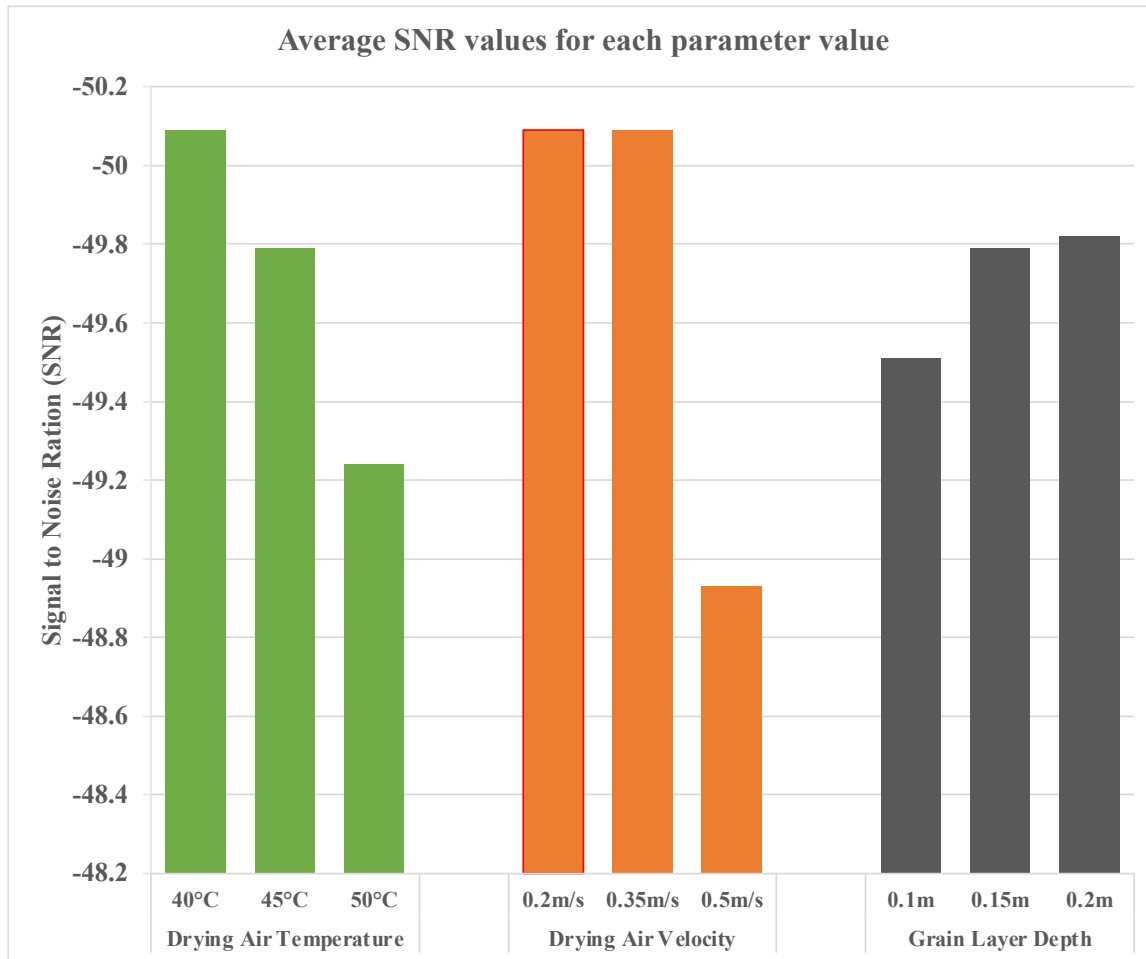


**Figure 4.12: Average SNR for individual parameters at each level**

The calculated results were verified using the main effects plots in figure 4.13 from Minitab 20 which indicated the highest mean SNR values for the three levels of drying air temperature, drying air velocity, and grain layer depth were level 3, 3, and 1 respectively. Therefore, the optimal combination for minimum total drying time is 50°C drying air temperature, 0.5m/s drying air velocity, and 0.1m grain layer depth.

From the results, a temperature of 50°C was the optimal level for drying maize in the geothermal dryer. This temperature is high enough to evaporate the moisture in the grain but not too high to

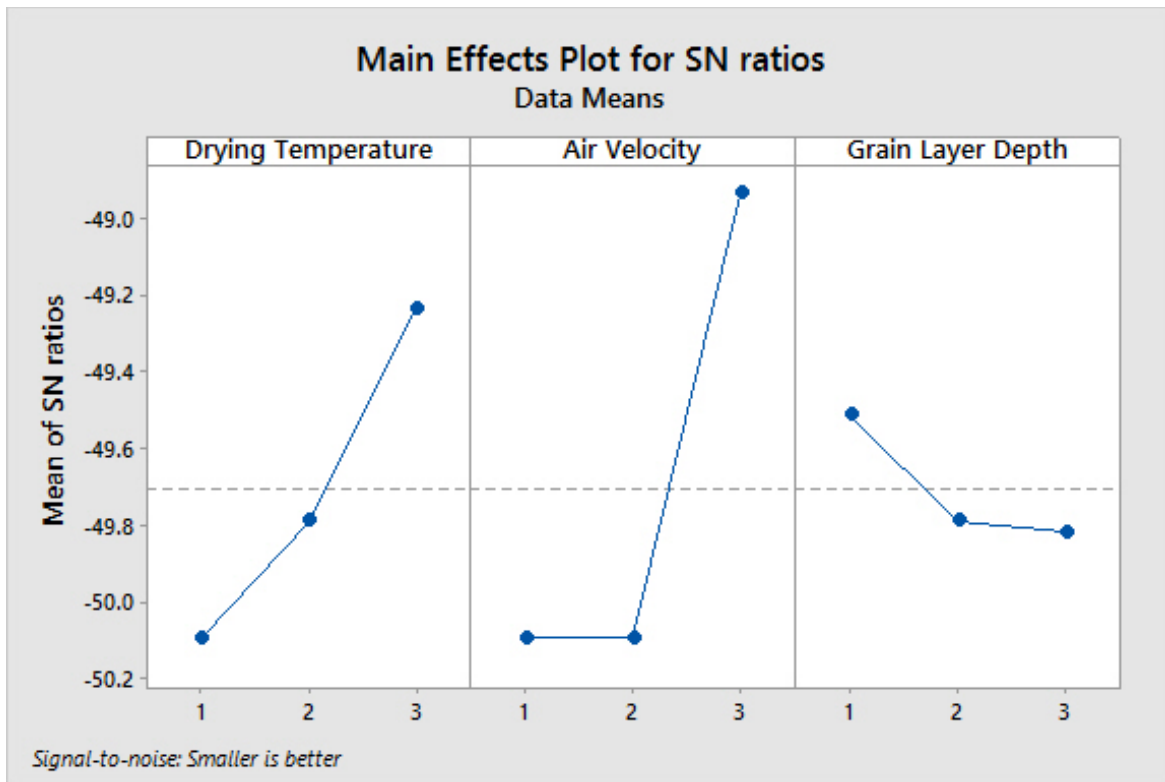


**Figure 4.13: Main effects plot for SNR for temperature, velocity, and grain depth**

cause damage to the maize grain. Higher temperatures may lead to over drying and cracking of the grains. Syariffuddeen et al. (2020) conducted a study which determined that drying maize above 50°C resulted in single and multiple stress cracking, which reduces the quality of the dried grains. Another research by Akowuah et al. (2018) focusing on kernel damage and grain quality determined that the optimal drying temperature of 50°C does not affect the quality and germination viability of maize grains. Also, a study by Abasi and Minaei (2014) to determine how the drying air temperature affected the quality of dried grains determined that an increase in the drying air temperature had resultant decrease in the drying time. Their research proposed that for maize meant for storage, lower temperatures of between 40°C and 50°C were recommended as this resulted in better grain quality.

The optimization results showed that air velocity of 0.5m/s was the optimal level for drying in the geothermal dryer. Similar research by Kinyanjui (2013) used a drying air velocity of 0.5m/s to design a geothermal maize dryer to successfully dry maize grains from 27% to 13%wb. These results are similar to the research by Pupinis (2008) on grain drying using comparative air flow, the researcher reported that air velocity of 0.15m/s to 0.42m/s had similar energy consumption but an increase in the air velocity beyond this point resulted in increased energy consumption for the grain dryer. Increasing air velocity helps increase the rate of moisture transfer from the grain to the surrounding air, and prevents moisture accumulation in the surrounding air, both of which contribute to reducing drying time. However, higher air velocities result in increased energy consumption and thus reduced energy efficiency. When the drying air velocity is too slow, it can result in extended drying times and a risk of grain spoilage from rewetting of the grains due to moisture accumulation.

The results of this study found that a grain depth of 0.1m was the optimal level for drying in the geothermal dryer. These results tally with the results of the experiment conducted by Osodo (2018) to assess how grain layer thickness affected the rate of moisture removal of maize and determined that the rate of moisture removal reduced with increase in grain layer depth due to increased drying air saturation. Similar research by Kajuna et al. (2001) on drying of cassava roots noted that a shallower layer of the cassava roots resulted in a shorter time in achieving the equilibrium moisture content of the cassava roots. This means that a shallow grain depth allows for more efficient airflow through the grain, which facilitates the removal of moisture. As air flows through the grain, it absorbs moisture and carries it away, but when grain layer is deep, the airflow is restricted and less effective in removing moisture.

Overall, the results indicate that the combination of 50°C temperature, 0.5m/s air velocity, and 0.1m grain depth provides the best conditions for drying in the geothermal dryer, resulting in the shortest drying time. This information is important in optimizing how to design and operate geothermal dryers efficiently and cost-effectively for drying maize grains.

#### **4.3.2 Analysis of Variance (ANOVA)**

ANOVA was conducted to determine whether the three variables, namely temperature, velocity, and grain layer depth significantly affected total drying time. Three-way ANOVA was conducted and the results showed no significant effects for temperature ( $F = 7.00$ ,  $p = 0.125$ ), velocity ( $F = 16.00$ ,  $p = 0.059$ ) or grain layer depth ( $F = 1.00$ ,  $p = 0.500$ ) (Appendix IIB, Table A3). However, as the p-value of velocity was marginally greater than 0.05, two-way ANOVA tests were performed.

Two-way ANOVA was performed with a combination of temperature and velocity on the drying time, temperature and grain layer depth, and velocity and grain layer depth on the drying time. Two-way ANOVA results of analyzing temperature and velocity effects on the drying time showed that both temperature [ $F(2,4)=7.00$ ,  $p=0.0494$ ] and velocity [ $F(2,4)=16.00$ ,  $p=0.0123$ ] significantly affected the drying time (Appendix IIB, Table A4). These results show that varying temperature and velocity can lead to significant changes on the drying time. The results of the two-way ANOVA analyzing the effects of velocity and grain layer depth on the drying time showed that velocity [ $F(2,4)=4.00$ ,  $p=0.111$ ] had a marginally significant effect on the drying time, while grain layer depth [ $F(2,4)=0.25$ ,  $p=0.790$ ] did not have a significant effect (Appendix IIB, Table A5). The results of the two-way ANOVA analyzing the temperature and grain layer depth effect on the drying time showed that neither temperature [ $F(2,4)=0.824$ ,

$p=0.502$ ] nor grain layer depth [ $F(2,4)=0.118$ ,  $p=0.892$ ] significantly affected the drying time (Appendix IIB, Table A6). The results showed that varying temperature and grain layer depth does not have a significant effect on the the drying time. These results show that varying velocity may have a moderate effect on the drying time , while varying grain depth does not appear to have a significant effect.

After establishing that varying temperature and velocity can lead to significant changes on the drying time, a Tukey's HSD post-hoc test was performed to examine which particular groups were significantly differed from each other. The post-hoc results established that there was a significant statistical difference between temperatures of  $50^{\circ}\text{C}$  and  $40^{\circ}\text{C}$  ( $p=0.045$ ). There is also a significant statistical difference between the drying air velocities of  $0.5\text{m/s}$  and  $0.2\text{m/s}$  ( $p=0.018$ ) and between air velocities of  $0.5\text{m/s}$  and  $0.35\text{m/s}$  ( $p=0.018$ ) (Appendix IIB, Table A7). The Tukey post-hoc test revealed that a temperature of  $50^{\circ}\text{C}$  resulted in reduced drying time than  $45^{\circ}\text{C}$  by 20 minutes; and similarly resulting in reduced drying time by 30 minutes than a temperature of  $40^{\circ}\text{C}$ . Also, increasing air velocity from both  $0.2\text{m/s}$  to  $0.35\text{m/s}$  and  $0.35\text{m/s}$  to  $0.5\text{m/s}$  resulted in reduced drying time by 40 minutes each. These results further support that the optimal temperature and air velocity from maize drying from the experiments were  $50^{\circ}\text{C}$  and  $0.5\text{m/s}$  respectively.

## CHAPTER FIVE: CONCLUSION AND RECOMMENDATIONS

### 5.1 Conclusion

A geothermal maize dryer with 0.55m (L) × 0.25m (W) × 1m (H) dimensions and a drying capacity of 40kg was designed, tested, and optimized for drying maize grains to a moisture content of 13% moisture content wet bulb in Menengai Menengai Geothermal Project Site in Nakuru County weather conditions. The dryer had an axial fan with a power rating of 0.035kW and a heat exchanger with overall heat transfer coefficient of 86.8 W/m<sup>2</sup>K.

Experiment evaluating the effect of drying air temperature on the total drying time showed that at 40°C, the total drying time taken to attain 13% wb moisture content was 5 ½ hours. The total drying time reduced to 5 hours after increasing the drying air temperature to 45°C. Increasing the drying air temperature to 50°C had no effect on the total drying time which remained at 5 hours. These results show that increasing the temperature from 40°C to 45°C has a direct effect of reducing the total drying time by 30 minutes. However, further increasing from 45°C to 50°C did not change the total time of drying which remained unchanged at 5 hours.

The experiments evaluating how drying air velocity affected the total time of drying established that at 0.2m/s air velocity the total drying time to attain 13% wb moisture content was 5 ½ hours. Increasing it to 0.35m/s reduced the total drying time to 5 hours while further increasing in the to 0.5m/s had an effect of a further reduction in the drying time to 4 ½ hours. Therefore, increasing the drying air velocity had an effect of reducing the total drying time.

The experiments evaluating how grain layer depth affected the total drying time determined that at 0.1m depth, the total time for drying required to attain a moisture content of at least 13% wb was 4 ½ hours. When the grain layer depth was increased to 0.15m, the total drying time increased to 5 hours. Further increase in the grain layer depth to 0.2m did not change the total drying time

which remained at 5 hours. Therefore, the minimum drying time of 4 ½ hours was achieved with a grain depth of 0.1m while a drying time of 5 hours was achieved with grain depths of 0.15m and 0.2m. Therefore, as the grain depth was increased the drying time increased from 4 ½ hours at 0.1m to 5 hours with grain depths of both 0.15m and 0.2m.

Results for selecting the optimum parameters showed that the best combination to achieve minimum drying time using the Taguchi Method were 0.1m grain layer depth, 50°C drying air temperature, and 0.5m/s drying air velocity for the geothermal dryer. The performance analysis of this geothermal dryer provided valuable insights on its potential to the small-scale maize farmers within the community who can take advantage of the geothermal resources. This is a viable option for localized grain processing by efficiently handling small maize grain batch sizes to improve storage longevity.

## **5.2 Recommendations**

1. The findings of this study can be adopted by farmers, agribusinesses, and policymakers to promote sustainable maize drying using geothermal energy. Government incentives and regulatory support can facilitate adoption, while agribusinesses can integrate geothermal drying to reduce energy costs.
2. Further research on the energy efficiency of the geothermal dryer can be explored.
3. Further research can be focused on how the drying process impacts the nutritional value of dried maize grains.

## REFERENCES

- Abasi, S., & Minaei, S. (2014). Effect of drying temperature on mechanical properties of dried corn. *Drying technology*, 32(7), 774-780.
- Abd, A. A., Kareem, M. Q., & Naji, S. Z. (2018). Performance analysis of shell and tube heat exchanger: Parametric study. *Case studies in thermal engineering*, 12, 563-568.
- Abueluor, A. A., Amin, M. T., Abuelnour, M. A., & Younis, O. (2023). A comprehensive review of solar dryers incorporated with phase change materials for enhanced drying efficiency. *Journal of Energy Storage*, 72, 108425.
- Akhtaruzzaman, M., Mondal, M. H. T., Biswas, M., Sheikh, M. A. M., Khatun, A. A., & Sarker, M. S. H. (2021). Evaluation of drying performance, energy consumption, and quality of two-stage dried maize grain. *Journal of Biosystems Engineering*, 46(2), 151-162.
- Akowuah, J., Maier, D., Opit, G., McNeill, S., Amstrong, P., Campabadal, C., ... & Obeng-Akrofi, G. (2018). Drying temperature effect on kernel damage and viability of maize dried in a solar biomass hybrid dryer.
- Akpan, G. E., Onwe, D. N., Fakayode, O. A., & Offiong, U. D. (2017). Design and Development of an Agricultural and Bio-materials Cabinet Tray Dryer. *Science Research*, 4(6), 174.
- Amantéa, R. P., Fortes, M., Ferreira, W. R., & Santos, G. T. (2018). Energy and exergy efficiencies as design criteria for grain dryers. *Drying Technology*, 36(4), 491-507.
- Bagaskara, A., Al Asyari, M. R., Adityatama, D. W., Purba, D., Ahmad, A. H., Rizky, A., ... & Mukti, A. W. (2023). Exploring New Ideas to Promote and Improve Geothermal Direct Use in Indonesia. In *Proceedings, 48th Workshop on Geothermal Reservoir Engineering Stanford University*.

- De Groote, H., Akoko, P. O., Stroshine, R., Gathungu, E., & Ricker-Gilbert, J. (2023). Technical performance and economic efficiency of small-scale maize dryers in Kenya. *Journal of Stored Products Research*, *103*, 102158.
- Dorfeshan, M., & Mehrzad, S. (2023). Pneumatic dryers. In *Drying Technology in Food Processing* (pp. 157-173). Woodhead Publishing.
- GDC, (2010). Retrieved July 15, 2020, from <https://www.gdc.co.ke/menengai.php>
- Ghijis, M., Mortier, S., Cappuyns, P., Gernaey, K. V., De Beer, T., & Nopens, I. (2017). Extension of a mechanistic model for drying of single pharmaceutical granules to semi-continuous fluid bed drying. In *2017 AIChE Annual meeting*.
- Groote, H. D., Githinji, P. G., Munya, B. G., & Ricker-Gilbert, J. E. (2019). Economics of open-air maize drying in East Africa.
- Helvacı, H. U., Keles, N., & Akkurt, G. G. (2023). Energy and exergy analysis of a geothermal energy sourced hot-air drying system. *International Journal of Exergy*, *41*(1), 1-19.
- Hoffmann, V., Alonso, S., & Kang'ethe, E. (2023). Food safety in Kenya: Status, challenges, and proposed solutions. *Food Systems Transformation in Kenya*, 105.
- Hunter, M. C., Kemanian, A. R., & Mortensen, D. A. (2021). Cover crop effects on maize drought stress and yield. *Agriculture, Ecosystems & Environment*, *311*, 107294.
- Jia, D., Cathary, O., Peng, J., Bi, X., Lim, C. J., Sokhansanj, S., ... & Tsutsumi, A. (2015). Fluidization and drying of biomass particles in a vibrating fluidized bed with pulsed gas flow. *Fuel Processing Technology*, *138*, 471-482.

- Joshi, A., VikfigonoKsh, Sethi, S., Arora, B., Baruah, D., Narola, A., & Uhre, S. B. (2024). Drying of Horticultural Produce: Mechanization, Challenges, and Opportunities. *Advances in Postharvest and Analytical Technology of Horticulture Crops*, 83-103.
- Joshi, M., Kumar, N., & Baredar, (2019). P. Optimization of Solar Dryer using Taguchi Method.
- Kabeyi, M. J. B., & Olanrewaju, O. A. (2021, March). Development of a cereal grain drying system using internal combustion engine waste heat. In *11th annual international conference on industrial engineering and operations management Singapore*.
- Kajuna, S. T. A. R., Silayo, V. C. K., Mkenda, A., & Makungu, P. J. J. (2001). Thin-layer drying of diced cassava roots. *African Journal of Science and Technology*, 2(2).
- Khamala, A. S. (2016). *Drying Of Agricultural Products By Geothermal Heat In Kenya* (Master's thesis).
- Kinyanjui, S. (2013). Direct Use Of Geothermal Energy In Menengai, Kenya: Proposed Geothermal Spa And Crop Drying. *Geothermal Training Programme Reports 2013 Orkustofnun Grensasvegur 9 IS-108 Reykjavik Iceland*.
- Kulundu, L., Ndiritu, H., Kituu, G., & Kimotho, J. (2022). Performance simulation of a modified geothermal grain dryer based at Menengai Well 3 in Kenya. *World Journal of Engineering and Technology*, 10(1), 59-87.
- Lund, J. W., Hutterer, G. W., & Toth, A. N. (2022). Characteristics and trends in geothermal development and use, 1995 to 2020. *Geothermics*, 105, 102522.
- Majdi, H., & Esfahani, J. A. (2019). Energy and drying time optimization of convective drying: Taguchi and LBM methods. *Drying Technology*, 37(6), 722-734.
- Mrema, J. C., Gumbe, L. O., Chepete, H. J., & Agullo, J. O. (2011). Grain crop drying, handling and storage. *Rural Structures in the Tropics: Design and Development*, 363-386.

- Njoroge, A. W., Baoua, I., & Baributsa, D. (2019). Postharvest management practices of grains in the Eastern region of Kenya. *Journal of Agricultural Science*, 11(3).
- Onyango, S. O. (2015). *Design of Steam Gathering System for Menengai Geothermal Field, Kenya* (Doctoral dissertation).
- Osodo, B. O. (2018). Simulation and Optimisation of a Drying Model for a Forced Convection Grain Dryer. *Unpublished PhD Thesis, Kenyatta University, Kenya*.
- Öztürk, Y., & Çobanoğlu, F. (2023). The Effect of Activities intended for Obtaining Geothermal Energy on Agricultural Production Systems. *Tarım Ekonomisi Araştırmaları Dergisi*, 9(1), 1-13.
- Popovska-Vasilevska, S. (2003). Drying of agricultural products with geothermal energy. *International Summer School on Direct Application of Geothermal Energy, Doganbey (Izmir), Turkey*, 2-15.
- Pupinis, G. (2008). Grain Drying by use of changeable air flow method. *Institute of Agricultural Engineering, Agronomy Research, ISSN*, 55-65.
- Sadaka, S. (2014). *Selection, performance and maintenance of grain bin fans*. Cooperative Extension Service, University of Arkansas.
- Sadaka, S. (2022). Impact of grain layer thickness on rough rice drying kinetics parameters. *Case Studies in Thermal Engineering*, 35, 102026.
- Sao, J. K., Naayagi, R. T., Panda, G., Patidar, R. D., & Swain, S. D. (2022). SAPF Parameter Optimization with the Application of Taguchi SNR Method. *Electronics*, 11(3), 348.
- Sarker, A., Islam, M. N., & Shaheb, M. R. (2012). A study on the drying behaviour of a local variety (Lalpakri) of potato (*Solanum tuberosum* L.). *Bangladesh Journal of Agricultural Research*, 37(3), 505-514.

- Sharmin, T., Khan, N. R., Akram, M. S., & Ehsan, M. M. (2023). A state-of-the-art review on geothermal energy extraction, utilization, and improvement strategies: conventional, hybridized, and enhanced geothermal systems. *International Journal of Thermofluids*, 18, 100323.
- Simiyu, S. M. (2010, April). Status of geothermal exploration in Kenya and future plans for its development. In *Proceedings world geothermal congress* (pp. 25-29).
- Sontakke, M. S., & Salve, S. P. (2015). Solar drying technologies: A review. *International Journal of Engineering Science*, 4(4), 29-35.
- Stephen, A. K., & Emmanuel, S. (2009). Improvement on the design of a cabinet grain dryer. *American Journal of Engineering and Applied Sciences*, 2(1), 217-228.
- Stutt, R. O., Castle, M. D., Markwell, P., Baker, R., & Gilligan, C. A. (2023). An integrated model for pre-and post-harvest aflatoxin contamination in maize. *npj Science of Food*, 7(1), 60.
- Sumotarto, U. (2007). Design of a geothermal energy drier for beans and grains drying in Kamojang Geothermal Field, Indonesia. *GHC Bulletin*, 28, 13-18.
- Syariffuddeen, A., Yahya, S., Ruwaida, A. W., Zainun, M. S., Shahrir, A., Azman, H., ... & Shanmugevelu, S. (2020). Evaluation on Drying Temperature of Grain Corn and Its Quality using Flat-bed Dryer.
- Tonui, K. S., Mutai, E. B. K., Mutuli, D. A., Mbugue, D. O., & Too, K. V. (2014). *Design and evaluation of solar grain dryer with a back-up heater*.
- Twidell, J., & Weir, T. (2015). *Renewable energy resources*. Routledge.
- Welty, J., Rorrer, G. L., & Foster, D. G. (2014). *Fundamentals of momentum, heat, and mass transfer*. John Wiley & Sons.

**APPENDICES**

**Appendix I: Results of Dryer Performance**

**Table A1: Temperature Variations for Unloaded Dryer**

| <b>Time (Minutes)</b> | <b>Inlet (Ambient) Temperature (°C)</b> | <b>Cabinet Temperature (°C)</b> |
|-----------------------|---|---------------------------------|
| 0                     | 22.3                                    | 24.3                            |
| 30                    | 22.9                                    | 41.6                            |
| 60                    | 23.5                                    | 48.3                            |
| 90                    | 23.9                                    | 52.1                            |
| 120                   | 24.8                                    | 54.3                            |
| 150                   | 25                                      | 55.5                            |
| 180                   | 25.1                                    | 55.9                            |
| 210                   | 25.2                                    | 56                              |
| 240                   | 25.3                                    | 56                              |
| 270                   | 25.2                                    | 56                              |
| 300                   | 25.2                                    | 56                              |

**Table A2: Volumetric Flow Rate to Vary Cabinet Temperature at different Velocities**

| <b>At 0.2m/s Air Velocity</b>  |  |   |   |
|--------------------------------|--|---|---|
| <b>Experiment</b>              | <b>Volumetric flow rate of Geothermal-heated water (L/s)</b> | <b>Inlet (Ambient) Temperature (°C)</b> | <b>Average Cabinet Temperature (°C)</b> |
| <b>1</b>                       | 0.21   | 24.3                                    | 40                                      |
| <b>2</b>                       | 0.32   | 24.5                                    | 45                                      |
| <b>3</b>                       | 0.54   | 23.9                                    | 50                                      |
| <b>At 0.35m/s Air Velocity</b> |  |   |   |
| <b>Experiment</b>              | <b>Volumetric flow rate of Geothermal-heated water (L/s)</b> | <b>Inlet (Ambient) Temperature (°C)</b> | <b>Average Cabinet Temperature (°C)</b> |
| <b>4</b>                       | 0.47   | 23.8                                    | 40                                      |
| <b>5</b>                       | 0.59   | 24.4                                    | 45                                      |
| <b>6</b>                       | 0.71   | 24.1                                    | 50                                      |
| <b>At 0.5m/s Air Velocity</b>  |  |   |   |
| <b>Experiment</b>              | <b>Volumetric flow rate of Geothermal-heated water (L/s)</b> | <b>Inlet (Ambient) Temperature (°C)</b> | <b>Average Cabinet Temperature (°C)</b> |
| <b>7</b>                       | 0.74   | 24.3                                    | 40                                      |
| <b>8</b>                       | 0.88   | 24.6                                    | 45                                      |
| <b>9</b>                       | 1.02   | 23.9                                    | 50                                      |

**Table A3: Measurement Results for Effect of Drying Air Temperature**

| Experiment | Total Drying Time<br>(Minutes) to achieve MC<br>of below 13% wb | Moisture Content<br>(%wb) |       | Weight (Kg) |       |
|------------|---|---------------------------|-------|-------------|-------|
|            |   | Initial                   | Final | Initial     | Final |
| 1          | 330   | 19.3                      | 12.9  | 28.7        | 25    |
| 2          | 300   | 19.4                      | 13    | 28.7        | 25.3  |
| 3          | 300   | 19.3                      | 12.9  | 28.8        | 25.5  |

**Table A4: Measurement Results for Effect of Drying Air Velocity**

| Experiment | Total Drying Time<br>(Minutes) to<br>achieve MC of<br>below 13% wb | Moisture Content<br>(%wb) |       | Weight (Kg) |       |
|------------|--|---------------------------|-------|-------------|-------|
|            |  | Initial                   | Final | Initial     | Final |
| 1          | 330  | 19.3                      | 13    | 28.4        | 24.5  |
| 2          | 300  | 19.4                      | 13    | 28.6        | 24.7  |
| 3          | 270  | 19.4                      | 12.9  | 28.5        | 24.9  |

**Table A5: Measurement Results of the Effect of Grain Layer Depth**

| Experiment | Total Drying<br>Time (Minutes)<br>to achieve MC<br>of below 13%<br>wb | Moisture Content<br>(%wb) |       | Weight (Kg) |       |
|------------|---|---------------------------|-------|-------------|-------|
|            |   | Initial                   | Final | Initial     | Final |
| 1          | 270   | 19.3                      | 13    | 18.1        | 15.5  |
| 2          | 300   | 19.4                      | 13    | 28.6        | 24.8  |
| 3          | 300   | 19.3                      | 13    | 36.7        | 32.1  |

**Appendix II: Dryer Optimization**

**Appendix IIA: Taguchi Design**

**Table A1: Drying times for the L9 Orthogonal Array Experiments**

| Experiment | Actual Values of Parameter/ Levels |                                 |                             | Total Drying Time<br>(Minutes) to achieve<br>MC of below 13%<br>wb |
|------------|------------------------------------|---------------------------------|-----------------------------|--|
|            | Drying Air<br>Temperature<br>(°C)  | Drying Air<br>Velocity<br>(m/s) | Grain<br>Layer<br>Depth (m) |  |
| 1          | 40                                 | 0.2                             | 0.10                        | 330  |
| 2          | 40                                 | 0.35                            | 0.15                        | 330  |
| 3          | 40                                 | 0.5                             | 0.20                        | 300  |
| 4          | 45                                 | 0.2                             | 0.15                        | 330  |
| 5          | 45                                 | 0.35                            | 0.20                        | 330  |
| 6          | 45                                 | 0.5                             | 0.10                        | 270  |
| 7          | 50                                 | 0.2                             | 0.20                        | 300  |
| 8          | 50                                 | 0.35                            | 0.10                        | 300  |
| 9          | 50                                 | 0.5                             | 0.15                        | 270  |

**Table A2: Average SNR for individual parameters at each level**

| Level | Drying Air Temperature | Drying Air Velocity | Grain Layer Depth |
|-------|------------------------|---------------------|-------------------|
| 1     | -50.09                 | -50.09              | -49.51            |
| 2     | -49.79                 | -50.09              | -49.79            |
| 3     | -49.24                 | -48.93              | -49.82            |

**Appendix IIB: ANOVA Results**

**Table A3: Three-Way ANOVA for Drying Time**

|             |        |         |         |             |
|-------------|--------|---------|---------|-------------|
| Df          | Sum Sq | Mean Sq | F value | Pr(>F)      |
| TEMPERATURE | 2      | 1400    | 700     | 7 0.1250    |
| VELOCITY    | 2      | 3200    | 1600    | 16 0.0588 . |
| GRAIN_DEPTH | 2      | 200     | 100     | 1 0.5000    |
| Residuals   | 2      | 200     | 100     |             |

---

Signif. codes: 0 '\*\*\*' 0.001 '\*\*' 0.01 '\*' 0.05 '.' 0.1 ' ' 1

**Table A4: Two-Way ANOVA for Drying Time (Temperature and Velocity)**

| Df          | Sum Sq | Mean Sq | F value | Pr(>F)      |
|-------------|--------|---------|---------|-------------|
| TEMPERATURE | 2      | 1400    | 700     | 7 0.0494 *  |
| VELOCITY    | 2      | 3200    | 1600    | 16 0.0123 * |
| Residuals   | 4      | 400     | 100     |             |

---

Signif. codes: 0 '\*\*\*' 0.001 '\*\*' 0.01 '\*' 0.05 '.' 0.1 ' ' 1

**Table A5: Two-Way ANOVA for Drying Time (Velocity and Grain Layer Depth)**

| Df          | Sum Sq | Mean Sq | F value | Pr(>F)     |
|-------------|--------|---------|---------|------------|
| VELOCITY    | 2      | 3200    | 1600    | 4.00 0.111 |
| GRAIN_DEPTH | 2      | 200     | 100     | 0.25 0.790 |
| Residuals   | 4      | 1600    | 400     |            |

**Table A6: Two-Way ANOVA for Drying Time (Temperature and Grain Layer Depth)**

| Df          | Sum Sq | Mean Sq | F value | Pr(>F)      |
|-------------|--------|---------|---------|-------------|
| TEMPERATURE | 2      | 1400    | 700     | 0.824 0.502 |
| GRAIN_DEPTH | 2      | 200     | 100     | 0.118 0.892 |
| Residuals   | 4      | 3400    | 850     |             |

**Table A7: Tukey's HSD Results**

\$TEMPERATURE

| diff  | lwr | upr       | p adj                |
|-------|-----|-----------|----------------------|
| 45-40 | -10 | -39.09985 | 19.0998464 0.5014690 |
| 50-40 | -30 | -59.09985 | -0.9001536 0.0454650 |
| 50-45 | -20 | -49.09985 | 9.0998464 0.1431828  |

\$VELOCITY

| diff     | lwr           | upr       | p adj               |
|----------|---------------|-----------|---------------------|
| 0.35-0.2 | 5.684342e-14  | -29.09985 | 29.09985 1.0000000  |
| 0.5-0.2  | -4.000000e+01 | -69.09985 | -10.90015 0.0175225 |
| 0.5-0.35 | -4.000000e+01 | -69.09985 | -10.90015 0.0175225 |

## Design and performance evaluation of a geothermal dryer for maize drying

Patrick Gitu<sup>1\*</sup>, Booker Osodo<sup>1</sup>, Willis Ambusso<sup>2</sup>

(1. Kenyatta University P.O Box 43844-00100 Nairobi, Department of Energy, Gas and Petroleum;

2. Kenyatta University P.O Box 43844-00100 Nairobi, Department of Physics)

**Abstract:** Exploiting geothermal energy to dry crops needs a properly designed geothermal crop dryer that is sized to meet the drying requirements of the crops to be dried. This study designed and fabricated a geothermal maize dryer that was tested to determine the drying time required to drying maize grains to 13% w.b. (wet basis) moisture content at Menengai Geothermal Project site within Nakuru County, Kenya. The main components of the geothermal dryer comprised of a dryer cabinet, heat exchanger, and fan unit. Once the air used for maize drying was heated by the heat exchanger, the sized fan unit blew hot air across the maize grains. Geothermal water from a discharging well within the project site supplied the heat to the sized heat exchanger. The designed geothermal maize dryer cabinet had dimensions of 0.55 m × 0.25 m × 1 m with 40 kg drying capacity, a 0.035 kW axial fan with a 0.035 kW motor, and a heat exchanger with an overall heat transfer coefficient of 86.8 W m<sup>-2</sup> K<sup>-1</sup>. The experimental results of the designed geothermal dryer showed that increasing the drying air temperature and drying air velocity inside the dryer resulted in reducing the total drying time while increasing the grain layer depth resulted in increased drying time. Experimental results revealed that the shortest drying time required to reduce the moisture content of maize from 19.3% w.b. to 12.9% w.b. was 4 ½ hours, achieved using a drying air temperature of 45°C, a drying air velocity of 0.5 m s<sup>-1</sup>, and a grain layer depth of 0.15 m. This is significantly lower than the average of 5 days it takes to dry maize in open-sun drying.

**Keywords:** geothermal dryer, maize drying, dryer cabinet, heat exchanger, fan unit, drying time

**Citation:** Gitu, P., B. Osodo, and W. Ambusso. 2024. Design and performance evaluation of a geothermal dryer for maize drying. *Agricultural Engineering International: CIGR Journal*, 26(1): 269-277.

### 1 Introduction

Drying agricultural products is a traditional method for preserving various foods like grains, meat, and fish. Since most farm products are not consumed immediately after harvesting, post-harvest processing such as drying is necessary (Popovska-Vasilevska, 2003). Food drying helps to lower the moisture content of the food products, which provides

numerous benefits such as extended shelf life, minimized risk of aflatoxin formation, and decreased mold growth. It also helps in reducing transportation and storage costs.

In general, the drying process involves the transfer of heat and mass water. The drying air is heated and then blown over the product to be dried. The heat then conducts inward through the product, which raises the temperature of the product continuously until the moisture at the product surface starts to evaporate. As the heated air continuously blows over the product to be dried, it absorbs moisture from the surface of the product and carries it away, maintaining a constant supply of dry air for

Received date: 2023-08-12 Accepted date: 2023-11-07

\*Corresponding author: Patrick Gitu, Engineer, Kenyatta University P.O Box 43844-00100 Nairobi, Department of Energy, Gas and Petroleum P.O Box 43844-00100 Nairobi. Tel:+254722913161, E-mail:kanjukigitu@gmail.com.



# Optimization of a Geothermal Maize Dryer for Minimum Drying Time

Patrick Gitu<sup>1</sup> · Booker Osodo<sup>1</sup> · Willis Ambusso<sup>2</sup>

Received: 9 February 2024 / Accepted: 12 July 2024  
© Indian National Academy of Engineering 2024

## Abstract

Efficient drying of maize plays a crucial role in preserving its quality and ensuring food security. This study investigated the performance of an experimental geothermal maize dryer under various drying conditions and optimized its parameters for improved drying time. The objective was to identify the best combination of drying air velocity, air temperature, and grain layer depth using the Taguchi method implemented in Minitab 20 statistical software. Analysis of Variance (ANOVA) was conducted using R-4.2.3 software to test the significance of varying the selected parameters on the drying time. Tukey's Honestly Significant Difference (Tukey's HSD) was used to establish whether the relationship between two sets of selected parameters was statistically significant. The selected parameters were varied within predetermined ranges to assess their individual and combined effects on the drying time of the geothermal maize dryer. Results for the optimal combination of parameters using the Taguchi Method found the optimal combination to be a drying air temperature of 50°C, a drying air velocity of 0.5 m/s, and a grain depth of 0.1 m, resulting in the minimum drying time. ANOVA and Tukey's HSD analysis confirmed there was a significant effect on the drying time when velocity and temperature were varied. Optimal parameter values can serve as practical guidelines for designing and operating geothermal maize dryers to reduce drying time.

**Keywords** Geothermal maize dryer · Optimization · Drying time · Taguchi method

## Introduction

As a major staple food in Kenya, maize has a key role in ensuring the food security of the nation (Groote et al. 2019). However, despite its significance, Kenya faces substantial post-harvest losses during maize storage, estimated at around 30%. As a result, post-harvest losses are a significant contributor to food insecurity in Kenya and the Sub-Saharan countries. One of the main factors in post-harvest losses is inappropriate or improper drying of the maize (Kimiye 2015). Drying harvested grains is crucial to prevent loss during the period between harvest and consumption. Maize has a moisture content ranging between 20 and 25% wet basis (wb) at the time of harvesting, which is ideal for

fungal and insect damage (Gitonga et al. 2013). Since this high moisture can damage the maize grains, reducing the moisture content through drying to around 11–13% is essential to facilitate longer-term storage of the maize (Folaranmi 2008). During the drying process, there is a transfer of both mass and heat between the product undergoing drying and the surrounding medium (Abdullah and Gunadnya 2010). Besides aiding in food preservation, drying of agricultural farm products improves food security (Andritsos et al. 2003). Further, dried food products result in weight reduction making it easier to transport.

Drying methods range from traditional open-air sun drying to mechanized drying (Helvacı 2012). As one of the earliest methods of drying farm products, open-air sun drying is the most common method because of its ease of use, which simply involves direct exposure of agricultural farm products to sunlight and wind to remove moisture. (Sontakke and Salve 2015). Although it is popular, it is very challenging since it has a very low rate of moisture removal, it needs a lot of space to lay the grains, and it requires dedicated manual labour (Ogheneruona and Yusuf 2011). Additionally, grains dried through this process are at high risk of spoilage

✉ Patrick Gitu  
kanjukigitu@gmail.com

<sup>1</sup> Department of Energy, Gas and Petroleum Engineering, Kenyatta University, P.O. Box 43844-00100, Nairobi, Kenya

<sup>2</sup> Department of Physics, Kenyatta University, P.O. Box 43844-00100, Nairobi, Kenya

#### **Appendix IV: Definition of Terminologies**

**Fluid Friction** – The resistance encountered by a fluid (liquid or gas) as it flows over a surface or through a conduit, which affects the efficiency of fluid movement in systems such as dryers and heat exchangers.

**Geothermal Brine** – A high-temperature, mineral-rich fluid extracted from geothermal reservoirs, often used for energy generation and direct applications such as heating and drying in industrial and agricultural processes.

**Geothermal Energy** – Heat energy derived from the Earth's interior, used for power generation and direct applications like drying agricultural products.

**Heat Transfer Coefficient** – A measure of the heat transfer capability of a material or system, indicating how effectively heat is transferred from one medium to another.

**Optimum Parameters** – The specific set of conditions or variables that yield the best performance or results in a given process or system.

**Psychrometrics** – The study of the thermodynamic properties of moist air, including temperature, humidity, vapor pressure, and enthalpy.

**Specific Heat Capacity** – The amount of heat required to raise the temperature of a unit mass of a substance by one degree Celsius, important for understanding energy requirements in drying.

**Thermal Conductivity** – A measure of a material's ability to conduct heat, influencing the efficiency of heat transfer within the dryer.

**Void Space** – The unoccupied space within the dryer cabinet that can be filled with air or another fluid.

## Appendix V: Research Authorization



### KENYATTA UNIVERSITY GRADUATE SCHOOL

E-mail: [dean-graduate@ku.ac.ke](mailto:dean-graduate@ku.ac.ke)

P.O. Box 43844, 00100

Website: [www.ku.ac.ke](http://www.ku.ac.ke)

NAIROBI, KENYA  
Tel. 020-8704150

#### Internal Memo

**FROM:** Dean, Graduate School

**DATE:** 7<sup>th</sup> July, 2021

**TO:** Mr. Patrick Kanjuki Gitu  
C/o Department of Energy Technology

**REF:** J104/26619/2018

**SUBJECT: APPROVAL OF RESEARCH PROPOSAL**

=====  
This is to inform you that Graduate School Board, at its meeting on 25<sup>th</sup> June, 2021, approved your Research Proposal for the M.Sc. Degree entitled, "Sizing, Testing and Optimization of a Geothermal Maize Dryer."

You may now proceed with your Data collection, subject to clearance with the Director General, National Commission for Science, Technology & Innovation.

As you embark on your data collection, please note that you will be required to submit to Graduate School completed Supervision Tracking and Progress Report Forms per semester. The forms are available at the University's Website under Graduate School webpage downloads.

Thank you.

**EDWIN OBUNGU**  
**FOR: DEAN, GRADUATE SCHOOL**

CC. Chairman, Department of Energy Technology

**Supervisors:**

1. Dr. Booker Onyango Osodo  
C/o Energy Technology Department  
Kenyatta University
2. Prof. Willis Jakanyango Ambusso  
C/o Physics Department  
Kenyatta University



REPUBLIC OF KENYA



NATIONAL COMMISSION FOR SCIENCE, TECHNOLOGY & INNOVATION

Ref No: 146093

Date of Issue: 27/September/2023

RESEARCH LICENSE



This is to Certify that Mr.. Patrick Kanjuki Gitu of Kenyatta University, has been licensed to conduct research as per the provision of the Science, Technology and Innovation Act, 2013 (Rev.2014) in Nakuru on the topic: SIZING, TESTING AND OPTIMIZATION OF A GEOTHERMAL MAIZE DRYER for the period ending : 27/September/2024.

License No: NACOSTI/P/23/29843

146093

Applicant Identification Number

*Walter*

Director General  
NATIONAL COMMISSION FOR SCIENCE, TECHNOLOGY & INNOVATION

Verification QR Code



NOTE: This is a computer generated License. To verify the authenticity of this document, Scan the QR Code using QR scanner application.

See overleaf for conditions